UCLouvain
Institute of Mechanics,
Materials and Civil Engineering

Robust optimisation of the pathway towards a sustainable whole-energy system

A hierarchical multi-objective reinforcement-learning based approach

Doctoral dissertation presented by
Xavier RIXHON

in partial fulfillment of the requirements for
the degree of Doctor in Engineering Sciences

December 2023

Thesis committee
Pr. Francesco CONTINO (supervisor, UCLouvain)
Pr. Hervé JEANMART (supervisor, UCLouvain)
Dr. Stefano MORET (ETH Zurich)
Pr. Sylvain QUOILIN (ULiège)

Abstract

This thesis will be awesome

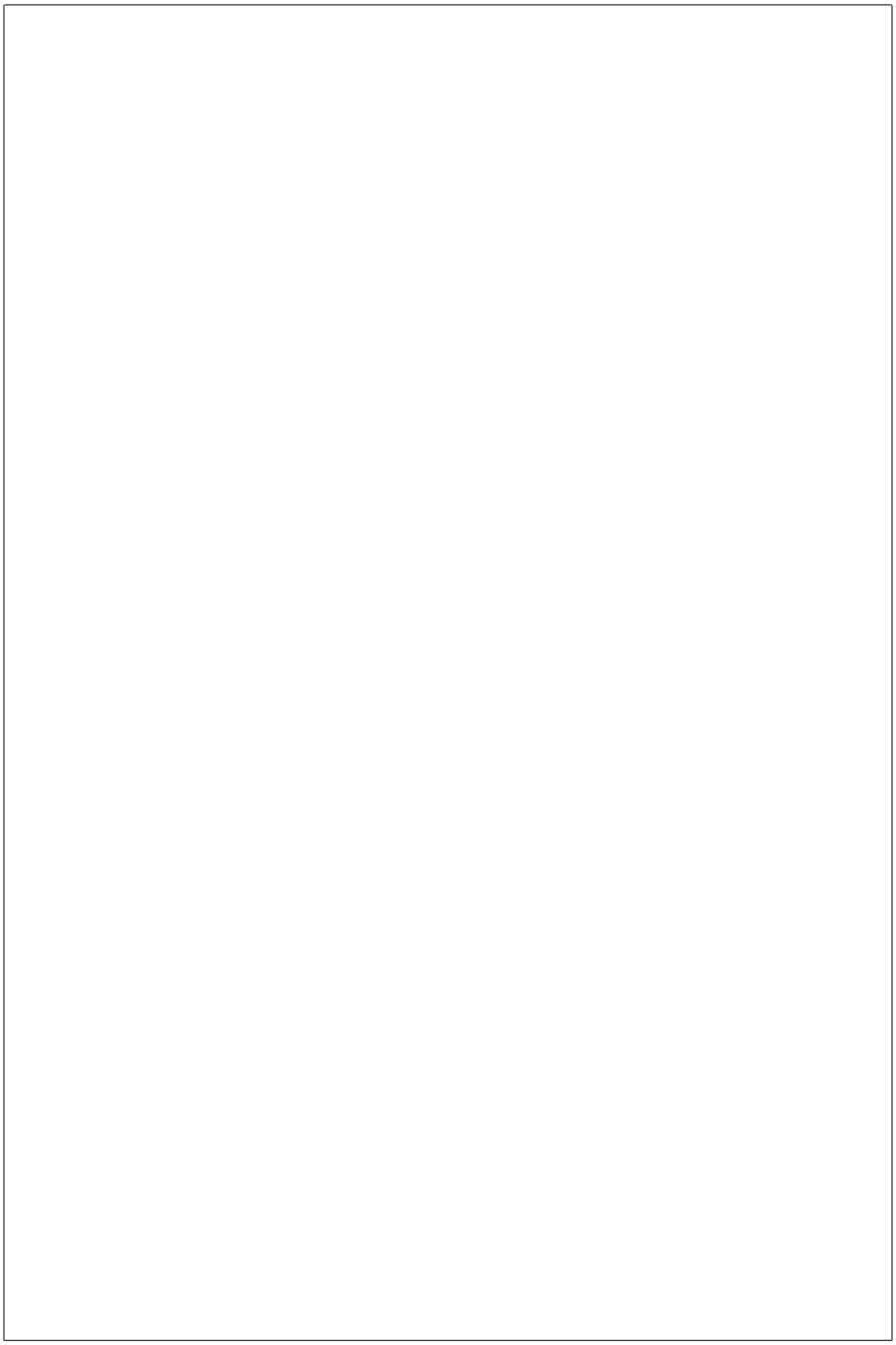

“Pour ce qui est de l’avenir, il ne s’agit pas de le prévoir,
mais de le rendre possible”

– Antoine de Saint Exupéry, Citadelle, 1948

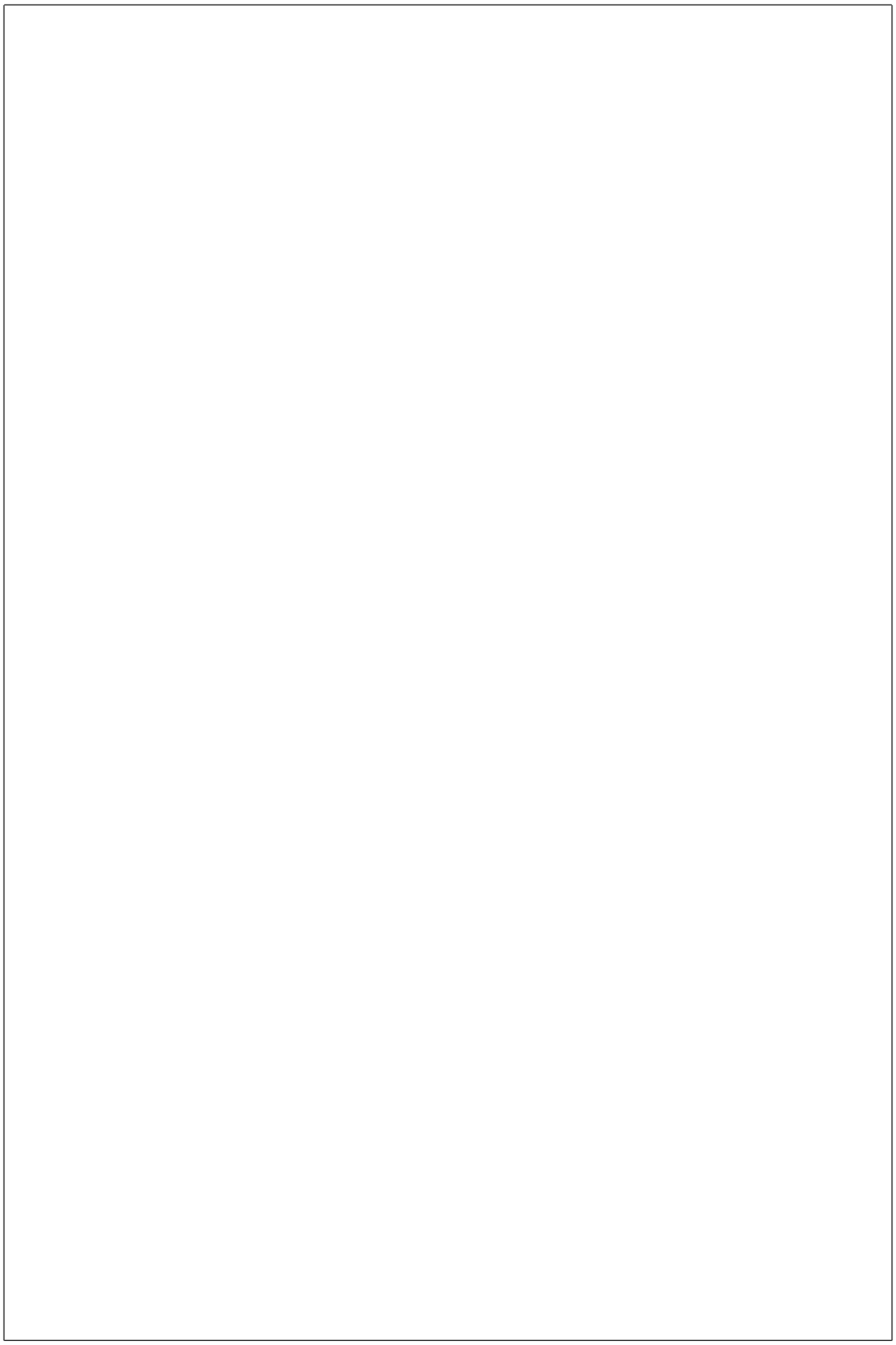

Remerciements

Thank you, thank you, far too kind

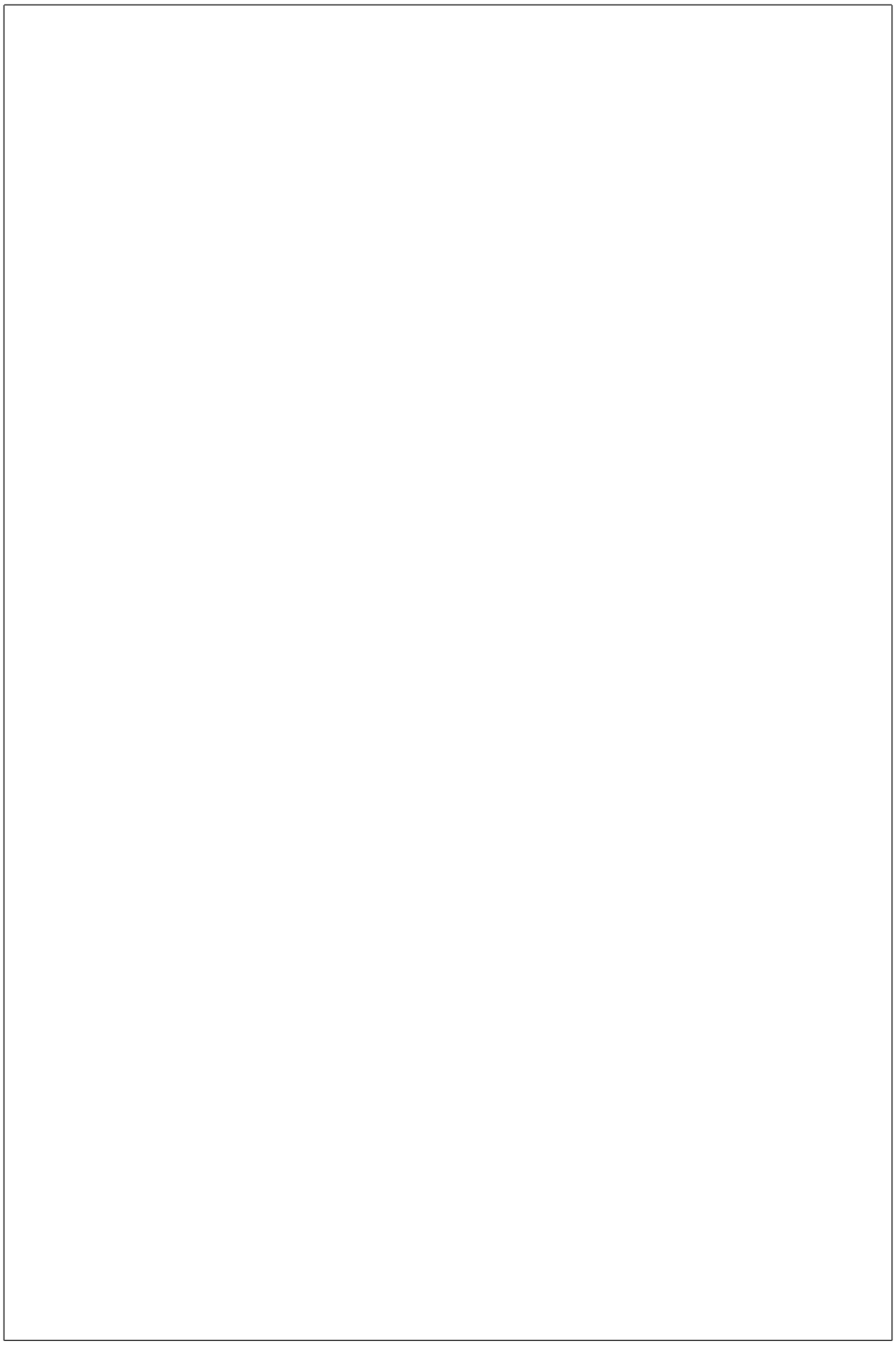

Contents

Symbols

Acronyms

BEV	battery electric vehicle
BTX	benzene, toluene and xylene
CAPEX	capital expenditure
CCGT	combined cycle gas turbine
CHP	combined heat and power
DHN	district heating network
EnergyScope TD	EnergyScope Typical Days
EUD	end-use demand
FC	fuel cell
GHG	greenhouse gases
GWP	global warming potential
HP	heat pump
HVC	high value chemicals
IEA	International Energy Agency
IPCC	intergovernmental panel for climate change
LCA	life cycle assessment
LCOE	levelised cost of energy
LFO	light fuel oil
LOO	leave-one-out
LPG	liquefied petroleum gas
MMSA	Methanol Market Services Asia
MTBE	methyl tert-butyl ether
NED	non-energy demand
NG	natural gas
NRE	non-renewable energy

NSC	naphtha steam cracker
OPEX	operational expenditure
PCE	Polynomial Chaos Expansion
PV	photovoltaic
RE	renewable energy
SDGs	Sustainable Development Goals
SMR	small modular reactor
UQ	Uncertainty Quantification

List of publications

Limpens, G., **Rixhon, X.**, Contino, F., & Jeanmart, H. (2024). "*EnergyScope Pathway: An open-source model to optimise the energy transition pathways of a regional whole-energy system.*" In Applied Energy, (Vol. 358). URL: https://doi.org/10.1016/j.apenergy.2023.122501

Rixhon, X., Limpens, G., Coppitters, D., Jeanmart, H.,& Contino, F.(2022). "*The role of electrofuels under uncertainties for the Belgian energy transition.*" In Energies (Vol. 14). URL: https://doi.org/10.3390/en14134027

Rixhon, X., Limpens, G., Contino, F., & Jeanmart, H. (2021). "*Taxonomy of the fuels in a whole-energy system.*" In Frontiers in Energy Research, Sec. Sustainable Energy Systems, (Vol. 9). URL: https://doi.org/10.3389/fenrg.2021.660073

Rixhon, X., Tonelli, D., Colla, M., Verleysen, K., Limpens, G., Jeanmart, H. ,& Contino, F.(2022). "*Integration of non-energy among the end-use demands of bottom-up whole-energy system models.*" In Frontiers in Energy Research, Sec. Process and Energy Systems Engineering, (Vol. 10). URL: https://doi.org/10.3389/fenrg.2022.904777

Rixhon, X., Colla, M., Tonelli, D., Verleysen, K., Limpens, G., Jeanmart, H., & Contino, F.(2021). "*Comprehensive integration of the non-energy demand within a whole-energy system: Towards a defossilisation of the chemical industry in Belgium.*" In proceedings of ECOS 2021 conference (Vol. 34, p. 154).

Limpens, G., Coppitters, D., **Rixhon, X.**, Contino, F., & Jeanmart, H. (2020). "*The impact of uncertainties on the Belgian energy system: application of the Polynomial Chaos Expansion to the EnergyScope model.*" In proceedings of ECOS 2020 conference (Vol. 33, p. 711).

Chapter 1

Methodology: Through a variety of complementary tools

1.1 Contributions

- Apply Stefano's method on the pathway model with a similar approach as Guevara et al.
- Check that PCE was appropriate as a method for such a system (ECOS2020)
- Work on the C_inv_return

Other authors' main contribution statement

On top of the main contributions of this thesis that are aforementioned, three main authors are to be mentioned for having brought a significant part of the methodological work. Based on Stefano Moret's monthly whole-energy system model (i.e. EnergyScope) [1], Gauthier Limpens has developed the hourly version of the snapshot model (i.e. EnergyScope TD) [2], as well as the perfect foresight pathway model [3], to which I personally contributed too. Diederik Coppitters has developed the RHEIA framework allowing to quantify the impact of uncertainties and carry out robust optimisation of energy systems [4]. The current work used this framework for the first of these functionalities. Finally, Stefano Moret extensively assessed the uncertainty characterisation on the Swiss energy system [5]. This thesis follows the same methodology, updating the uncertainty ranges for the pathway model.

1.2 Whole-energy system transition model optimisation: EnergyScope Pathway

On the contrary, this work optimises the entire transition pathway from a known system in 2020 up to 2050 thanks to EnergyScope Pathway [3]. According to pathway models review (see Appendix A.1), EnergyScope Pathway can be categorised as an investment and operation optimisation model that assesses the whole-energy system, has a hourly time-resolution and is open-source documented model. Moreover, it maintains a low computational cost (i.e. around 15 minutes for a 30-year pathway with a hourly discretisation). From the perfect to the myopic foresight of the transition optimisation, this section presents only the main constraints of the model. The reader is invited to refer to Appendix A.2 for more details about the formulation of the model and its extension from a snapshot approach, EnergyScope TD. More extensive information about the formulation choices, for instance, can be found in [3] and the documentation [6].

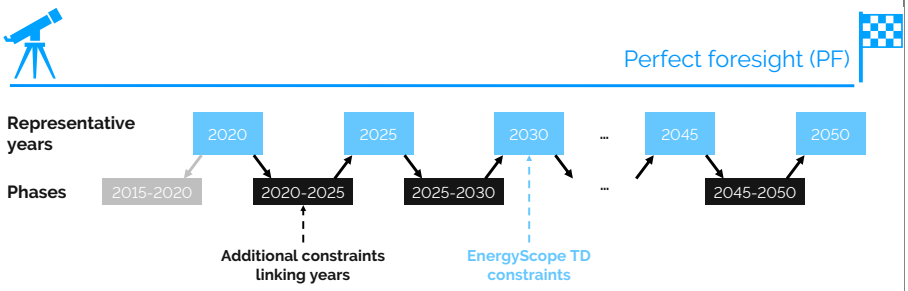

Figure 1.1. Illustration of the pathway methodology based on an existing energy system model. The methodology spans from 2020 to 2050, with one representative year every five years. The model EnergyScope Typical Days (EnergyScope TD) is applied in 7 representative years (light blue boxes). The formulation includes additional constraints (black boxes) that link the years together. The pathway's initialisation assumes that all capacities installed in 2020 were built during the pseudo-phase of 2015-2020 (grey box). The overall problem is defined as the pathway model.

We used the perfect foresight (PF) formulation (Figure 1.1)—the entire transition is computed in one optimisation, assuming a complete but uncertain knowledge of the different parameters until 2050. Even though this lacks realism compared to the myopic approach [7–9] where the pathway is optimised via a sequence of shorter time windows, the perfect foresight approach allows to optimise the transition with a CO_2-

budget (Section **??**) rather than along a prescribed CO_2-trajectory. However, the work of Limpens et al. [3] has shown that PF provides similar results for the study case compared to the myopic approach with a prescribed linear decrease of the CO_2-emissions . All the variables and constraints of the snapshot model, EnergyScope TD [2], are kept as is with an extra-dimension to relate them to a specific representative year, y, of the pathway. For instance, the energy balance is guaranteed at every hour of each of these years.

The optimised objective of the pathway model, i.e. the total transition cost $\mathbf{C_{tot,trans}}$, is computed as follows:

$$\min \ \mathbf{C_{tot,trans}} = \mathbf{C_{tot,capex}} + \mathbf{C_{tot,opex}} \tag{1.1}$$

$$\mathbf{C_{tot,capex}} = \sum_{p \in PHASE \cup \{2015\_2020\}} \mathbf{C_{inv,phase}}(p) - \sum_{j \in TECH} \mathbf{C_{inv,return}}(j) \tag{1.2}$$

$$\mathbf{C_{tot,opex}} = \mathbf{C_{opex}}(2020) + t_{phase} \cdot \tau_{phase}(p) \cdot \sum_{p \in PHASE | y_{\text{start}} \in P\_START(p), y_{\text{stop}} \in P\_STOP(p)} \left(\mathbf{C_{opex}}(y_{\text{start}}) + \mathbf{C_{opex}}(y_{\text{stop}}) \right) / 2 \tag{1.3}$$

$$\tau_{phase}(p) = 1/(1 + i_{rate})^{diff\_2015\_year(p)} \tag{1.4}$$

where $t_{phase} = 5$ years and *diff_2015_year(p)* are respectively the duration of a phase between two representative years and the number of years between the middle of a phase and 2015 for a correct annualisation. $\mathbf{C_{inv,return}}$ accounts for the residual value, also called *salvage value*, of the technologies installed during the transition and having not reached the end of their lifetime by 2050. This last variable is crucial to avoid penalising heavy (and potentially long-lifetime) investments at the end of the transition as these assets would still be operational beyond 2050. The interested reader will find more information about its implementation and the formulation choices related to it in the work of Limpens et al. [3]. The other variables in Eq. (1.2-A.18) are detailed here below:

$$\mathbf{C_{opex}}(y) = \sum_{j \in TECH} \mathbf{C_{maint}}(y, j) + \sum_{i \in RES} \mathbf{C_{op}}(y, i) \qquad \forall y \in YEARS \tag{1.5}$$

$$\mathbf{C_{inv,phase}}(p) = \sum_{j \in TECH} \mathbf{F_{new}}(p, j) \cdot \tau_{phase}(p) \cdot \left(c_{inv}(y_{start}, j) + c_{inv}(y_{stop}, j) \right) / 2 \qquad \forall p \in PHASE | y_{\text{start}} \in P\_START(p), y_{\text{stop}} \in P\_STOP(p) \tag{1.6}$$

where $\mathbf{F_{new}}$ are the capacities newly installed. In Eq. (A.20-A.21), the costs related to each representative year are:

$$\mathbf{C_{inv}}(y,j) = c_{inv}(y,j)\mathbf{F}(y,j) \qquad \forall y \in YEARS, \forall j \in TECH \quad (1.7)$$

$$\mathbf{C_{maint}}(y,j) = c_{maint}(y,j)\mathbf{F}(y,j) \qquad \forall y \in YEARS, \forall j \in TECH \quad (1.8)$$

$$\mathbf{C_{op}}(y,i) = \sum_{t \in T} c_{op}(y,i)\mathbf{F_t}(y,i,t)t_{op}(t) \qquad \forall y \in YEARS, \forall i \in RES \quad (1.9)$$

where the variable $\mathbf{F}$ represents the size of the installed capacities (for all technologies j) and the variable $\mathbf{F_t}$ is the hourly consumption of the resources; the parameters c_{inv} and c_{maint} are the CAPEX and the OPEX of the technologies, and the parameter c_{op} is the cost of purchasing resources. For the sake of simplicity, as done by Limpens et al. [3], the sum over the 8760 hours of the year is written as the sum over $t \in T$.

Then, as detailed in section **??**, the CO_2-budget for the transition, $\mathbf{GWP_{tot,trans}}$, is computed and constrained as follows:

$$\mathbf{GWP_{tot,trans}} = \mathbf{GWP_{tot}}(2020) + t_{phase} \sum_{p \in PHASE | y_{\text{start}} \in Y\_START(p), y_{\text{stop}} \in Y\_STOP(p)} \left(\mathbf{GWP_{tot}}(y_{\text{start}}) + \mathbf{GWP_{tot}}(y_{\text{stop}}) \right) / 2 \quad (1.10)$$

$$\mathbf{GWP_{tot,trans}} \leq gwp_{lim,trans} \quad (1.11)$$

where the computation of the yearly emissions are based on the global warming potential (GWP) of the resources:

$$\mathbf{GWP_{tot}}(y) = \sum_{i \in RES} \mathbf{GWP_{op}}(y,i) \qquad \forall y \in YEARS \quad (1.12)$$

$$\mathbf{GWP_{op}}(y,i) = \sum_{t \in T} gwp_{op}(y,i)\mathbf{F_t}(y,i,t)t_{op}(t) \qquad \forall y \in YEARS, \forall i \in RES \quad (1.13)$$

where gwp_{op} is the specific emissions (i.e. in $kt_{CO_2,eq}$/GWh) of each resource. Based on an approach developed by the Intergovernmental Panel on Climate Change (IPCC) [10], this work considers the indicator "GWP100a - IPCC2013" to compute the emissions related to the use of resources. This includes the emissions due to the extraction, the transportation and the combustion of the energy carrier. EnergyScope proposes to account for the embodied emissions of the technologies based on a life cycle assessment (LCA). These stand for extraction of materials, refining, construction and end of life [11]. However, this work is still in progress and the database is not yet complete. Consequently, it is not included in this work and not accounted for.

Besides this constraint on the emissions, the main constraint to link years with each other is the one dictating the installed capacities at the end of each year:

$$\mathbf{F}(y_{\text{stop}}, j) = \mathbf{F}(y_{\text{start}}, j) + \mathbf{F_{new}}(p, j) - \mathbf{F_{old}}(p, j) - \sum_{p2 \in PHASE \cup \{2015\_2020\}} \mathbf{F_{decom}}(p, p2, j)$$

$$\forall p \in PHASE, y_{stop} \in Y\_STOP(p), y_{start} \in Y\_START(p), j \in TECH \quad (1.14)$$

where the variables $\mathbf{F_{old}}$ and $\mathbf{F_{decom}}$ are the capacities respectively having reached the end of their lifetime and prematurely decommissioned. Moreover, to account for the society inertia and to prevent unrealistically fast modal share change, constraints limit this change for the sectors of the low-temperature, the passenger mobility and freight mobility demands. The parameters $\Delta_{\text{change,LT\_heat}}$, $\Delta_{\text{change,pass}}$ and $\Delta_{\text{change,freight}}$ respectively limit their respective modal share change up to 33%, 50% and 50% per phase of 5 years.

1.3 Uncertainty quantification

1.3.1 Uncertainty characterisation

1.3.2 Polynomial Chaos Expansion

We used Polynomial Chaos Expansion (PCE), an approach for surrogate-assisted Uncertainty Quantification (UQ), to propagate uncertainties in input parameters through the system model. This allowed us to assess statistical moments on the quantity of interest and determine Sobol' indices [12]. To construct a PCE of the EnergyScope Pathway model, we employed the open-source Python framework RHEIA [13, 14]. Where the first part of this section is dedicated to the mathematical definition of this approach, the second details its choice and summarises the comparison made with another approach (i.e. Morris method) in a previous work [15].

Definition

The PCE model ($\hat{M}$) is a representation of the relationship between the input parameters and the output variable of interest (i.e. results) in the EnergyScope Pathway model (M). This representation is constructed as a truncated series of multivariate orthonormal polynomials $\mathbf{\Psi}$, weighted by coefficients u:

$$\hat{M}(\boldsymbol{\xi}) = \sum_{\boldsymbol{\alpha} \in \mathcal{A}^{d,p}} u_{\boldsymbol{\alpha}} \mathbf{\Psi}_{\boldsymbol{\alpha}}(\boldsymbol{\xi}) \approx M(\boldsymbol{\xi}), \quad (1.15)$$

where the vector $\boldsymbol{\xi} = (\xi_1, \xi_2, \dots \xi_d)$ comprises the independent random input parameters (section B.4), d corresponds to the number of input distributions and $\boldsymbol{\alpha}$ is a

multi-index, i.e. a vector of non-negative indices of length d, where each index corresponds to the degree of each univariate polynomial that forms the basis of the multivariate polynomial $\mathbf{\Psi}_{\boldsymbol{\alpha}}$. As uniform distributions are considered, the Legendre polynomials are adopted, as they are the associated family of polynomials that are orthogonal with respect to standard uniform distributions [16].

A truncation scheme is implemented to restrict the number of multivariate polynomials in the series. This is done based on two factors: a specified limiting polynomial order (p) and the number of uncertain parameters (d) involved. The multivariate polynomial order $|\boldsymbol{\alpha}|$ is the summation of the orders for each univariate polynomial in the multivariate polynomials space. Thus, only the multi-indices corresponding to an order that is less than or equal to the specified limiting order are retained and stored in the truncated series denoted as $\mathcal{A}^{d,p}$:

$$\mathcal{A}^{d,p} = \left\{ \boldsymbol{\alpha} \in \mathbb{N}^d \, : \, |\boldsymbol{\alpha}| \leq p \right\}. \tag{1.16}$$

The number of multi-indices satisfying this condition is as the cardinality of $\mathcal{A}$, i.e. the number of its elements:

$$\text{card}\left(\mathcal{A}^{d,p}\right) = \binom{p+d}{p} = \frac{(d+p)!}{d!p!} = P + 1. \tag{1.17}$$

The coefficients $(u_0, u_1, \ldots, u_{P+1})$ are quantified using a regression method applied to orthonormal polynomials [16]. To ensure a well-posed least-square minimisation, it is recommended to have a number of training samples at least twice the number of coefficients [16]. Therefore, $2\,(P+1)$ samples are evaluated in the system model, and the model response for each quantity of interest is recorded. To generate the training samples, the quasi-random Sobol' sampling technique is employed [17]. As a low-discrepancy sequence, this technique exhibits the main advantage to investigate efficiently and (almost) uniformly the hypercube of uncertainties, unlike uniformly distributed random numbers.

The process of defining the polynomial degree includes incrementally increasing it until a desired level of accuracy is achieved [13]. Starting with $p = 1$, a PCE is constructed and the leave-one-out (LOO) error is evaluated. If the LOO error is below a specified threshold, the corresponding polynomial order is considered sufficient for generating an accurate PCE. However, if the error exceeds the threshold, the order is increased, and additional samples are generated following the rule of Eq. (1.17).

For the specific study of this work, a polynomial order of 2 is necessary (with 1260 training samples as per Eq. (1.17)) to achieve a LOO error below 1 % for the total transition cost.

Lastly, the statistical moments can be analytically derived from the PCE coefficients, eliminating the need for further model evaluations. The mean μ and standard deviation σ are obtained as follows:

$$\mu = u_0, \tag{1.18}$$

$$\sigma^2 = \sum_{i \neq 0} u_i^2. \tag{1.19}$$

Furthermore, the Sobol' indices can also be determined analytically. The total-order Sobol' indices (S_i^T) assess the overall influence of a stochastic input parameter on the performance indicator, encompassing all possible interactions:

$$S_i^T = \sum_{\boldsymbol{\alpha} \in A_i^T} u_{\boldsymbol{\alpha}}^2 / \sum_{i=1}^{P} u_i^2 \qquad A_i^T = \{\boldsymbol{\alpha} \in A | \alpha_i > 0\}. \tag{1.20}$$

Here, A denotes the collection of all PCE coefficients, and α_i corresponds to the coefficient associated with the uncertain parameter i.

Comparison with a proven method

Besides being an in-house used method, an early step of this thesis consisted in assessing PCE with similar approach used in the literature [15].

After characterising the uncertainty ranges, Moret et al. [5] quantified the impact of these uncertainties on the snapshot model of EnergyScope, i.e. ranking them, using the Morris method [18]. This method, as a statistical analysis, relies on individually randomized one-factor-at-a-time designs. Given the d model parameters $\vec{\xi} = (\xi_1, \xi_2, ..., \xi_d)$, the first step of the method consists in generating independent random samples of $\vec{\xi}$ in a standardised and discretised p-level *region of experimentation*, ω. In this *region of experimentation*, each ξ_i, varying in the interval $[\xi_{i,min},\ \xi_{i,max}]$, can take a random discrete value as follows :

$$\xi_i = \xi_{i,min} + j \cdot \frac{1}{p-1} \left(\xi_{i,max} - \xi_{i,min}\right) \quad \text{with } j \in \{0, 1, ..., p-1\} \tag{1.21}$$

Then, given these random one-factor-at-a-time samples, Morris method defines, for a given set of $\vec{\xi}$, the elementary effect of the ith parameter (EE_i) as :

$$EE_i = \frac{M(\xi_1, \xi_2, ..., \xi_i + \Delta, ..., \xi_d) - M(\vec{\xi})}{\Delta} \tag{1.22}$$

where M is the objective function, $\vec{\xi} \in \omega$, except $\xi_i \leq 1 - \Delta$ and Δ is a set multiple of $1/(p-1)\left(\xi_{i,max} - \xi_{i,min}\right)$. As in other studies [5, 19, 20], we consider p as even and $\Delta = p/[2(p-1)]\left(\xi_{i,max} - \xi_{i,min}\right)$.

Finally, in order to evaluate the importance of the ith parameter over an output, Morris method relies on F_i, the distribution of r elementary effects. Computing the mean, $\mu_i = \mu(F_i)$, and the standard deviation, $\sigma_i = \sigma(F_i)$, of the F_i distribution, allows ranking the parameters based on their influence on the concerned output. Usually, in Morris method, p and r respectively get values as follows : $p \in \{4, 6, 8\}$ and $r \in [15; 100]$ depending on, d, the number of uncertain parameters. The higher this number is, the higher shall be, simultaneously, p and r. In the following comparative analysis, we set p and r to their maximum values, respectively 8 and 100 in order to get the most reliable parameters ranking.

Beyond the original Morris method, we used the standardized elementary effects, SEE_i, formulation [19], given by

$$SEE_i = EE_i \cdot \frac{\sigma(\xi_i)}{\sigma(M)}. \tag{1.23}$$

Among other things, the SEE allows comparing the influence of different inputs on the same output or compare the influence of a same parameter on different outputs, even if these parameters or outputs are significantly different in terms of variation range or average amplitude. Moreover, this standardized analysis does not require any additional model evaluations.
Therefore, in the following results, we rather use

$$\mu_i^* = \mu(|SF_i|) \tag{1.24}$$

to rank parameters among each other. In (1.24), SF_i is the distribution formed by the r standardized elementary effects, as done in Moret [20].

In [15], we have assessed the PCE approach, comparing the Top-14 most impacting parameters obtained from this approach with the one provided by the improved Morris method based on μ_i^*. Even if the output of each method does not have the same physical meaning, both methods can rank the parameters by their impact on the total annual cost of the energy system. Both rankings were very similar which validates the use of PCE in the rest of this work.

1.3.3 Preliminary screening and selection

1.4 Reinforcement learning

1.5 Principal Components Analysis

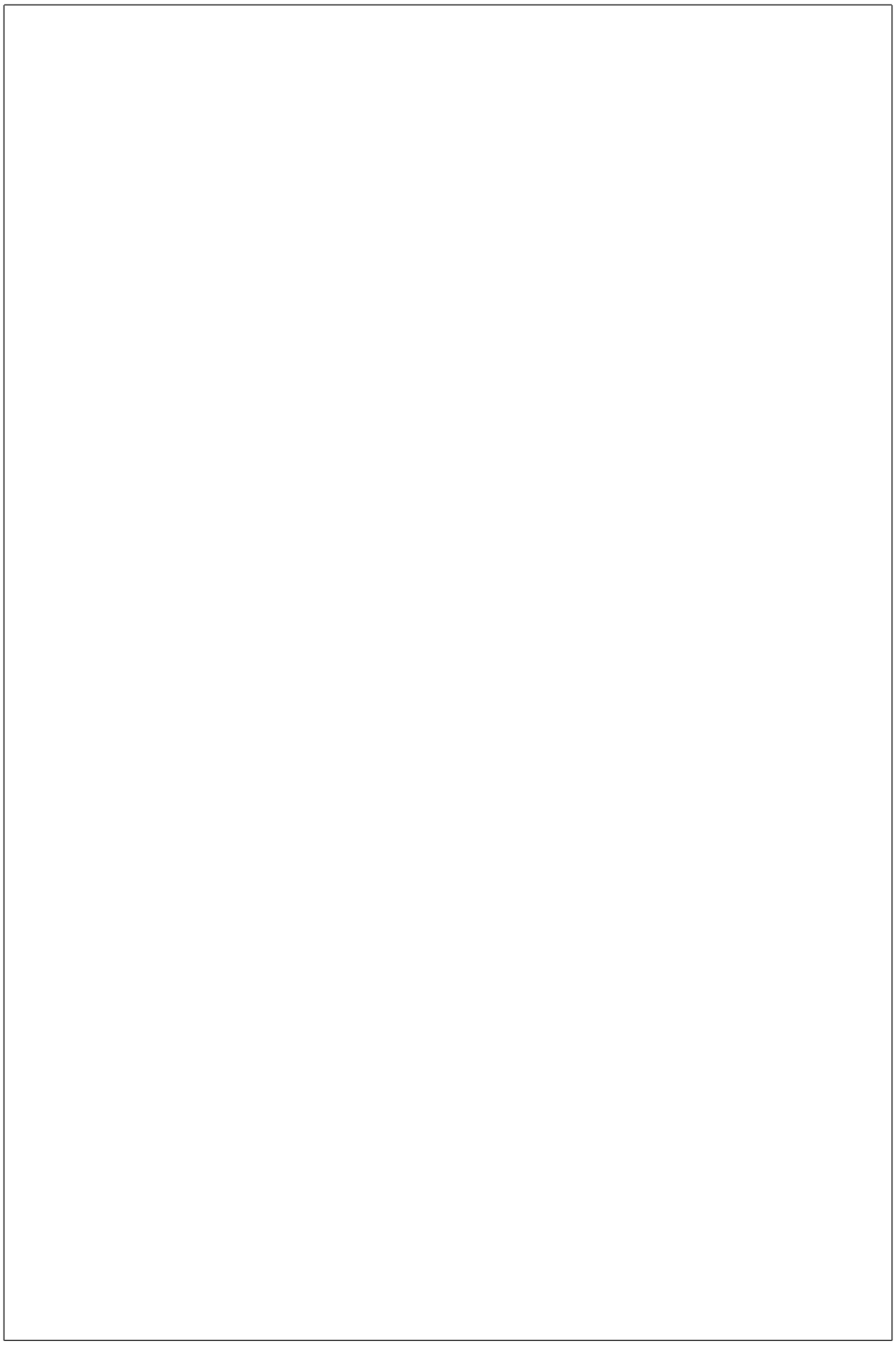

Bibliography

[1] S. Moret, M. Bierlaire, F. Maréchal, Strategic energy planning under uncertainty: a mixed-integer linear programming modeling framework for large-scale energy systems, in: Computer Aided Chemical Engineering, volume 38, Elsevier, 2016, pp. 1899–1904.

[2] G. Limpens, S. Moret, H. Jeanmart, F. Maréchal, Energyscope td: A novel open-source model for regional energy systems, Applied Energy 255 (2019) 113729.

[3] G. Limpens, X. Rixhon, F. Contino, H. Jeanmart, Energyscope pathway: an open-source model to optimise the energy transition pathways of a regional whole-energy system, Elsevier in Applied Energy (2024).

[4] D. Coppitters, Robust design optimization of hybrid renewable energy systems, Vrije Universiteit Brussel (VUB), University of Mons (UMONS), Mons (2021).

[5] S. Moret, V. Codina Gironès, M. Bierlaire, F. Maréchal, Characterization of input uncertainties in strategic energy planning models, Applied Energy 202 (2017) 597–617.

[6] G. Limpens, EnergyScope Pathway documentation, Accessed 2022. URL: `https://energyscope-pathway.readthedocs.io/en/v1.1/`.

[7] S. Babrowski, T. Heffels, P. Jochem, W. Fichtner, Reducing computing time of energy system models by a myopic approach: A case study based on the perseus-net model, Energy systems 5 (2014) 65–83.

[8] B. Fais, I. Keppo, M. Zeyringer, W. Usher, H. Daly, Impact of technology uncertainty on future low-carbon pathways in the uk, Energy Strategy Reviews 13 (2016) 154–168.

[9] C. F. Heuberger, I. Staffell, N. Shah, N. Mac Dowell, Impact of myopic decision-making and disruptive events in power systems planning, Nature Energy 3 (2018) 634–640.

[10] T. Stocker, Climate change 2013: the physical science basis: Working Group I contribution to the Fifth assessment report of the Intergovernmental Panel on Climate Change, Cambridge university press, 2014.

[11] J. Schnidrig, J. Brun, F. Maréchal, M. Margni, Integration of life cycle impact assessment in energy system modelling, Proceedings of ECOS 2023 (2023).

[12] D. Coppitters, W. De Paepe, F. Contino, Robust design optimization and stochastic performance analysis of a grid-connected photovoltaic system with battery storage and hydrogen storage, Energy 213 (2020) 118798.

[13] D. Coppitters, P. Tsirikoglou, W. D. Paepe, K. Kyprianidis, A. Kalfas, F. Contino, RHEIA: Robust design optimization of renewable Hydrogen and dErIved energy cArrier systems, Journal of Open Source Software 7 (2022) 4370. doi:10.21105/joss.04370.

[14] D. Coppitters, RHEIA documentation, Accessed 2022. URL: https://rheia.readthedocs.io/en/latest/index.html.

[15] G. Limpens, D. Coppitters, X. Rixhon, F. Contino, H. Jeanmart, The impact of uncertainties on the belgian energy system: Application of the polynomial chaos expansion to the energyscope model, Proceedings of the ECOS (2020).

[16] B. Sudret, Polynomial chaos expansions and stochastic finite element methods, Risk and reliability in geotechnical engineering (2014) 265–300.

[17] P. Bratley, B. Fox, Implementing sobols quasirandom sequence generator (algorithm 659), ACM Transactions on Mathematical Software 29 (2003) 49–57.

[18] M. D. Morris, Factorial Sampling Plans for Preliminary Computational Experiments, Technometrics 33 (1991) 161–174.

[19] G. Sin, K. V. Gernaey, Improving the morris method for sensitivity analysis by scaling the elementary effects, in: Computer Aided Chemical Engineering, volume 26, Elsevier, 2009, pp. 925–930.

[20] S. Moret, Strategic energy planning under uncertainty, Ph.D. thesis, EPFL, 2017.

[21] B. S. Palmintier, Incorporating operational flexibility into electric generation planning: Impacts and methods for system design and policy analysis, Ph.D. thesis, Massachusetts Institute of Technology, 2013.

[22] D. Connolly, H. Lund, B. V. Mathiesen, M. Leahy, A review of computer tools for analysing the integration of renewable energy into various energy systems, Applied Energy 87 (2010) 1059–1082. doi:10.1016/j.apenergy.2009.09.026.

[23] M. G. Prina, M. Lionetti, G. Manzolini, W. Sparber, D. Moser, Transition pathways optimization methodology through EnergyPLAN software for long-term energy planning, Applied Energy 235 (2019) 356–368. doi:10.1016/j.apenergy.2018.10.099.

[24] M. G. Prina, G. Manzolini, D. Moser, B. Nastasi, W. Sparber, Classification and challenges of bottom-up energy system models - a review, Renewable and Sustainable Energy Reviews 129 (2020) 109917.

[25] M. Chang, J. Z. Thellufsen, B. Zakeri, B. Pickering, S. Pfenninger, H. Lund, P. A. Østergaard, Trends in tools and approaches for modelling the energy transition, Applied Energy 290 (2021) 116731.

[26] R. Atlason, R. Unnthorsson, Ideal EROI (energy return on investment) deepens the understanding of energy systems, Energy 67 (2014) 241–245. doi:10.1016/j.energy.2014.01.096.

[27] Pfenninger and Pickering, Calliope - a multi-scale energy systems modelling framework, Accessed 2023. URL: https://www.callio.pe/.

[28] A. University, EnergyInteractive.NET, Accessed July 17th, 2018. URL: http://energyinteractive.net/.

[29] Ž. Popović, B. Brbaklić, S. Knežević, A mixed integer linear programming based approach for optimal placement of different types of automation devices in distribution networks, Electric Power Systems Research 148 (2017) 136–146.

[30] Berkeley Lab, Der-cam, Accessed June 12th, 2023. URL: https://gridintegration.lbl.gov/der-cam.

[31] A. Zerrahn, W.-P. Schill, Long-run power storage requirements for high shares of renewables: review and a new model, Renewable and Sustainable Energy Reviews 79 (2017) 1518–1534.

[32] University of Stuttgart, European Electricity Market Model, Accessed June 12th, 2023. URL: https://www.ier.uni-stuttgart.de/forschung/modelle/E2M2/.

[33] S. Backe, C. Skar, P. C. del Granado, O. Turgut, A. Tomasgard, Empire: An open-source model based on multi-horizon programming for energy transition analyses, SoftwareX 17 (2022) 100877.

[34] Quintel Intelligence, Energy transition model, Accessed September 17th, 2023. URL: https://docs.energytransitionmodel.com/main/intro/.

[35] H. Lund, J. Z. Thellufsen, Energyplan - advanced energy systems analysis computer model (version 15.1), https://doi.org/10.5281/zenodo.4001540, 2020. [Accessed September 17, 2020].

[36] O. Lugovoy, V. Potashnikov, energyRt: Energy systems modeling toolbox in R, development version, 2022. URL: https://github.com/energyRt/energyRt, r package version 0.01.21.9003.

[37] Freaunhofer ISI, Enertile, Accessed June 12th, 2023. URL: https://www.enertile.eu/enertile-en.

[38] C. F. Heuberger, Electricity systems optimisation with capacity expansion and endogenous technology learning (eso-xel), Zenodo (2017).

[39] K. Löffler, K. Hainsch, T. Burandt, P.-Y. Oei, C. Kemfert, C. Von Hirschhausen, Designing a model for the global energy system—genesys-mod: an application of the open-source energy modeling system (osemosys), Energies 10 (2017) 1468.

[40] H.-K. Bartholdsen, A. Eidens, K. Löffler, F. Seehaus, F. Wejda, T. Burandt, P.-Y. Oei, C. Kemfert, C. v. Hirschhausen, Pathways for germany's low-carbon energy transformation towards 2050, Energies 12 (2019) 2988.

[41] L. Herc, A. Pfeifer, F. Feijoo, N. Duić, Energy system transitions pathways with the new h2res model: a comparison with existing planning tool, e-Prime-Advances in Electrical Engineering, Electronics and Energy 1 (2021) 100024.

[42] M. G. Prina, D. Groppi, B. Nastasi, D. A. Garcia, Bottom-up energy system models applied to sustainable islands, Renewable and Sustainable Energy Reviews 152 (2021) 111625.

[43] R. Dufo López, ihoga, Accessed June 12th, 2023. URL: https://ihoga.unizar.es/en/.

[44] P. Kuhn, Iteratives Modell zur Optimierung von Speicherausbau und-betrieb in einem Stromsystem mit zunehmend fluktuierender Erzeugung, Ph.D. thesis, Technische Universität München, 2012.

[45] Electric Power Research Institute, Open distribution system simulator (opendss), Accessed June 12th, 2023. URL: https://sourceforge.net/projects/electricdss/.

[46] Energy Exemplar, Plexos (version 9.0), 2023. URL: https://plexos9.com/.

[47] V. Waucquez, Validation of the cost optimization model, pathway energyscope, for scenario analysis, 2023. URL: http://hdl.handle.net/2078.1/thesis:40534.

[48] T. Brown, J. Hörsch, D. Schlachtberger, Pypsa: Python for power system analysis, arXiv preprint arXiv:1707.09913 (2017).

[49] T. Brown, J. Hörsch, D. Schlachtberger, PyPSA: Python for Power System Analysis, 2018. URL: https://pypsa.org/.

[50] T. T. Pedersen, E. K. Gøtske, A. Dvorak, G. B. Andresen, M. Victoria, Long-term implications of reduced gas imports on the decarbonization of the european energy system, Joule 6 (2022) 1566–1580.

[51] Energistyrelsen, Modeldokumentation – Ramses energisystemmodel , Technical Report, 2023. URL: https://ens.dk/sites/ens.dk/files/Analyser/ramses_energisystemmodel.pdf.

[52] W. Short, P. Sullivan, T. Mai, M. Mowers, C. Uriarte, N. Blair, D. Heimiller, A. Martinez, Regional energy deployment system (ReEDS), Technical Report, National Renewable Energy Lab.(NREL), Golden, CO (United States), 2011.

[53] R. Loulou, U. Remme, A. Kanudia, A. Lehtila, G. Goldstein, Documentation for the times model part ii, Energy technology systems analysis programme (2005).

[54] IEA-ETSAP, Times model description, 2021. URL: https://wiki.openmod-initiative.org/wiki/TIMES.

[55] G. Haydt, V. Leal, A. Pina, C. A. Silva, The relevance of the energy resource dynamics in the mid/long-term energy planning models, Renewable energy 36 (2011) 3068–3074.

[56] S. Pfenninger, J. Keirstead, Renewables, nuclear, or fossil fuels? Scenarios for Great Britain's power system considering costs, emissions and energy security, Applied Energy 152 (2015) 83–93. doi:10.1016/j.apenergy.2015.04.102.

[57] B. Pickering, R. Choudhary, Quantifying resilience in energy systems with out-of-sample testing, Applied Energy 285 (2021) 116465.

[58] S. Pfenninger, Dealing with multiple decades of hourly wind and pv time series in energy models: A comparison of methods to reduce time resolution and the planning implications of inter-annual variability, Applied energy 197 (2017) 1–13.

[59] M. Welsch, P. Deane, M. Howells, B. Ó. Gallachóir, F. Rogan, M. Bazilian, H.-H. Rogner, Incorporating flexibility requirements into long-term energy system models–a case study on high levels of renewable electricity penetration in ireland, Applied Energy 135 (2014) 600–615.

[60] G. Limpens, Pathway extension of model EnergyScope TD, Accessed 2023. URL: https://github.com/energyscope/EnergyScope_pathway/tree/v1.1.

[61] V. Codina Gironès, S. Moret, F. Maréchal, D. Favrat, Strategic energy planning for large-scale energy systems: A modelling framework to aid decision-making, Energy 90, Part 1 (2015) 173–186. doi:10.1016/j.energy.2015.06.008.

[62] F. Contino, S. Moret, G. Limpens, H. Jeanmart, Whole-energy system models: The advisors for the energy transition, Progress in Energy and Combustion Science 81 (2020) 100872. URL: https://doi.org/10.1016/j.pecs.2020.100872.

[63] P. Thiran, H. Jeanmart, F. Contino, Validation of a method to select a priori the number of typical days for energy system optimisation models, Energies 16 (2023) 2772.

[64] X. Rixhon, G. Limpens, D. Coppitters, H. Jeanmart, F. Contino, The role of electrofuels under uncertainties for the belgian energy transition, Energies 14 (2021) 4027.

[65] G. Limpens, S. Moret, G. Guidati, X. Li, F. Maréchal, H. Jeanmart, The role of storage in the Swiss energy transition, in: proceedings of ECOS 2019 conference, 2019, pp. 761–774.

[66] G. Limpens, H. Jeanmart, F. Maréchal, Belgian energy transition: What are the options?, Energies 13 (2020) 261.

[67] M. Borasio, S. Moret, Deep decarbonisation of regional energy systems: A novel modelling approach and its application to the italian energy transition, Renewable and Sustainable Energy Reviews 153 (2022) 111730.

[68] J. Dommisse, J.-L. Tychon, Modelling of Low Carbon Energy Systems for 26 European Countries with EnergyScopeTD : Can European Energy Systems Reach Carbon Neutrality Independently?, Master's thesis, UCLouvain, 2020. URL: http://hdl.handle.net/2078.1/thesis:25202.

[69] M. Pavičević, P. Thiran, G. Limpens, F. Contino, H. Jeanmart, S. Quoilin, Bidirectional soft-linking between a whole energy system model and a power systems model, in: 2022 IEEE PES/IAS PowerAfrica, IEEE, 2022, pp. 1–5.

[70] J. Schnidrig, R. Cherkaoui, Y. Calisesi, M. Margni, F. Maréchal, On the role of energy infrastructure in the energy transition. case study of an energy independent and co2 neutral energy system for switzerland, Frontiers in Energy Research 11 (2023) 1164813. URL: https://doi.org/10.3389/fenrg.2023.1164813. doi:10.3389/fenrg.2023.1164813.

[71] G. Limpens, Generating energy transition pathways: application to Belgium, Ph.D. thesis, Université Catholique de Louvain, 2021.

[72] G. Limpens, EnergyScope TD documentation, Accessed 2023. URL: https://energyscope.readthedocs.io/en/v2.2/.

[73] IPCC, Climate Change 2013 - The Physical Science Basis, 2014. URL: https://www.ipcc.ch/report/ar5/wg1/.

[74] SPF Economie, Energy - key data - edition february 2022, Brussels, Februrary 2022.

[75] J. Mertens, R. Belmans, M. Webber, Why the carbon-neutral energy transition will imply the use of lots of carbon, C—Journal of Carbon Research 6 (2020) 39.

[76] D. Devogelaer, J. Duerinck, D. Gusbin, Y. Marenne, W. Nijs, M. Orsini, M. Pairon, "Towards 100% renewable energy in Belgium by 2050", Technical Report, 2013.

[77] M. Cornet, J. Duerinck, E. Laes, P. Lodewijks, E. Meynaerts, J. Pestiaux, N. Renders, P. Vermeulen, Scenarios for a Low Carbon Belgium by 2050, Technical Report November, Climact, VITO, 2013.

[78] Climact, VITO, New scenarios for a climate neutral Belgium by 2050, Technical Report, 2021. URL: `https://klimaat.be/doc/climate-neutral-belgium-by-2050-report.pdf`.

[79] Bureau Fédéral du Plan, Perspectives de l'évolution de la demande de transport en belgique à l'horizon 2030, 2015.

[80] Société Française d'énergie nucléaire, La belgique repousse de 10 ans sa sortie du nucléaire, `https://www.sfen.org/rgn/la-belgique-repousse-de-10-ans-sa-sortie-du-nucleaire/`, January 2023 (accessed April 17, 2023).

[81] EnergyVille, Paths2050 - the power of perspective, `https://perspective2050.energyville.be/`, 2022 (accessed December 2022).

[82] A. Dubois, J. Dumas, P. Thiran, G. Limpens, D. Ernst, Multi-objective near-optimal necessary conditions for multi-sectoral planning, arXiv preprint arXiv:2302.12654 (2023).

[83] Fédération Belge et Luxembourgeoise de l'automobile et du cycle, Automotive Pocket Guide Belgium - Chiffres clefs, Technical Report, 2021. URL: `https://www.febiac.be/public/statistics.aspx?FID=23`.

Appendix A

EnergyScope Pathway: Its choice and its formulation

A.1 EnergyScope Pathway: The right model to choose

Energy system models of varying complexity are valuable tools for guiding policy-makers and projecting future trends. These models enable the exploration of different energy scenarios and the assessment of their consequences based on the underlying assumptions. Specifically, techno-economic models play a crucial role in identifying technically feasible pathways for the energy transition while considering the associated economic costs. These models can be classified based on two key factors: technical resolution and simulation horizon, as illustrated in Figure A.1.

Increasing the technical resolution of energy system models often comes at the expense of a shorter simulation horizon, and vice versa. For instance, day-ahead grid operation models prioritise accurate grid resolution and capacity reserves for uncertainties, but they may not incorporate long-term market trends. Different model classes cater to various needs, with decreasing technical resolution. These include machine-level control, network dispatch, unit commitment, maintenance, power plant expansion, planning for new infrastructure, and scenario analysis. Each class serves a specific purpose, from fine-grained control within a machine to the exploration of multiple assumptions across different scenarios.

In accordance with the previous classification, models aimed at aiding decision-makers in the energy transition primarily fall under the categories of planning and scenario analysis, with a relatively lower technical resolution. Nonetheless, ensuring technical accuracy is of paramount importance to ensure the effective functionality of

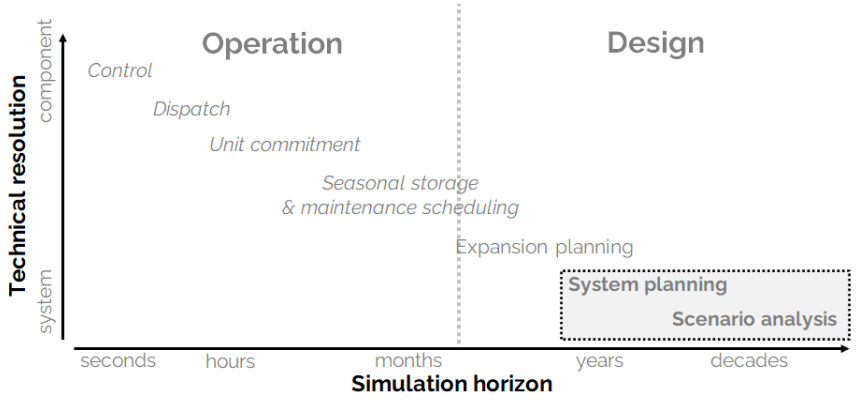

Figure A.1. Model can be classified by their core focus: **Operation** or **Design**. These categories can be broken down into subcategories. This paper focuses on the system planning and scenario analysis models. Inspired from [21].

future energy systems. Hence, these models should meet the following requirements as a minimum: (i) assessment of intermittent renewable energy integration; (ii) accounting for all energy flows in different sectors, including the measurement of greenhouse gas emissions in the energy sector; (iii) exploration of all available options; (iv) consideration of investments throughout the transition process; and (v) ensuring a reasonable computation time for analysing different trajectories. Additionally, to enhance result reproducibility and user understanding, it is advantageous for such models to: (vi) maintain transparency and preferably be open-source, accompanied by collaborative documentation.

These requirements can be transposed into criteria that a model should match: (i) it should have an hourly resolution spanning a one-year time horizon; (ii) it should encompass the entire energy system, including all types of demands (such as heat, electricity, mobility, and non-energy) , as well as all resources, conversion processes, and storage technologies; (iii) it should optimise the system design, accounting for all the options; (iv) it should have a long-term investment horizon, spanning several decades; (v) its computational time should be reasonable, typically less than one hour on a personal laptop; (vi) it should be open-source, with accessible data and comprehensive documentation. These requirements are commonly found in reviews of energy system models. In 2010, Connolly et al. [22] reviewed 68 tools, considering similar criteria: (i-iv) and (vi), along with others such as the number of users and market equilibrium. In 2019, Prina et al. [23] reviewed 12 "*most established*" models, focusing on criteria

(i-ii) and (iv). This review was followed by a classification where criteria (i-iv) were taken into account [24]. In 2021, Chang et al. [25] conducted a survey-based review of 42 models for energy transition modelling, covering all criteria except computational time. Based on these reviews, Tables A.1 and A.2 compare models based on all the previous criteria except the computational time (v). Indeed, the latter is hard to compare as models are not apply to the same case study and the information is rarely given. The table includes only the models that achieved partially at least four out of the five criteria. We endeavored to refresh the model's information by consulting the model's website and repository, yet there is a possibility that some information might have been overlooked or omitted inadvertently.

Table A.1. Comparison of existing models that partially satisfy at least four of the six criteria (in alphabetical order). Legend: ✓criterion satisfied; ✓ criterion partially satisfied; ✗ criterion not satisfied. Data from [22–25] (part A)

Model	Ref.	Hourly	Whole-energy	Optimis. invest. & operation	Pathway	Open-source
Calliope	[26, 27]	✓	✓	✓	✗[a]	✓
COMPOSE	[28]	✓	✓	✓	✓	✓[b]
DER-CAM	[29, 30]	✓	✓[c,d]	✓	✗[e]	✓[f]
DIETER	[31]	✓	✓[d,g]	✓	✗[e]	✓
E2M2	[32]	✓	✓[c,d,h]	✓	✓	✗[i]
EMPIRE	[33]	✓	✗[c,d,g,h]	✓	✓	✓[b]
Ener. Trans. Model	[34]	✓	✓	✗[j]	✓	✓
EnergyPLAN	[35]	✓	✓	✗[k]	✗[l]	✓[f]
energyRt	[36]	✓	✓	✓[m]	✓	✓
EnergyScope TD	[2]	✓	✓	✓	✗[l]	✓
Enertile	[37]	✓	✓[d]	✓	✓	✗[n]

[a] Topic is being discussed in the chat of their repository but not yet included in their documentation.
[b] '*Free under some special conditions´*.
[c] Transport not accounted.
[d] Industry not accounted
[e] Not specified but time horizon is 1 year.
[f] Freeware.
[g] district heating network (DHN) not accounted.
[h] individual heating not accounted.
[i] Commercially (paid) licensed.
[j] The ETM is a simulation model with a simple merit order 'optimisation' for electricity, flex and heat.
[k] Simulation model.
[l] Yearly horizon without pathway.
[m] EnergyRT optimises investments only.
[n] Only for internal use.

From Tables A.1 and A.2, four models almost check all the boxes (partially the pathway one): Calliope, GENeSYS-MOD, PyPSA and TIMES. The TIMES model,

Table A.2. Comparison of existing models that partially satisfy at least four of the six criteria (in alphabetical order). Legend: ✓criterion satisfied; ✓ criterion partially satisfied; ✗ criterion not satisfied. Data from [22–25] (part B)

Model	Ref.	Hourly	Whole-energy	Optimis. invest. & operation	Pathway	Open-source
ESO-XEL	[38]	✓	✗[a,b,c,d]	✓	✓	✓
GENeSYS-MOD	[39]	✓	✓	✓	✓[e]	✓
H2RES	[41]	✓	✗[f]	✓[f]	✓	✓
iHOGA	[43]	✓	✗[a,b,c,d]	✓ [g]	✓	✓ [h]
IMAKUS	[44]	✓	✓[a,b]	✓	✓	✗[i]
OpenDSS	[45]	✓	✓	✗ [j]	✓	✓
Plexos	[46]	✓	✓[k]	✓	✓	✗[i]
PyPSA	[48, 49]	✓	✓	✓	✓ [l]	✓
RamsesR	[51]	✓	✓[a,b,d]	✓	✓	✓
ReEDS	[52]	✗[m]	✓[b,c,d]	✓	✓	✓ [h]
TIMES	[53]	✓	✓	✓	✓	✓[n]

[a] Transport not accounted.
[b] Industry not accounted
[c] DHN not accounted.
[d] individual heating not accounted.
[e] Löffler et al. [39] applied a pathway transition, but the time resolution was increased to 12h and it uses 3 typical days over a year. Bartholdsen et al. [40] performed a multi-regional pathway (16 nodes) for the case of Germany from 2020 to 2050 with a time step of 5 years. However, the time resolution is 16 time slices representing 4 hours per day and one day per season.
[f] In their review in 2021, Prina et al. [42] classified H2RES as a simulation model on power sector only. In their work, Herc et al. [41] presented a new version of H2RES claiming to optimise the power system and partially represent other sectors. Their study applied the model to a transition pathway for Croatia. In the conclusion, it is claimed '*H2RES offers practically unlimited potential for functionality expansion since it is an open-source program´* which open the doors for future developments to encompass new features.
[g] iHOGA conducts optimisation and simulation without specifying timing or scope.
[h] '*Free under some special conditions´*.
[i] Commercially (paid) licensed.
[j] Simulation model.
[k] Does not account for all sectors but allow to implement them according to Waucquez [47].
[l] Pedersen et al. [50] applied PyPSA to a whole energy system split in 37 nodes. Using a myopic approach, the model optimises the energy transition with a 3-hours resolution).
[m] Seasonal time slice.
[n] Model is now open-source with limited access to data [54].

short for The Integrated MARKAL-EFOM System, is a well-established framework renowned for its capacity to generate comprehensive energy models. It encompasses a rich array of features, including support for multi-cell modeling, pathway analysis, full-scale representation of energy systems, and the consideration of market equilibrium dynamics, all of which facilitate thorough scenario exploration. This model has a widespread adoption and has been utilized by worldwide institutions such as the International Energy Agency (IEA) or technical ones such as VITO (Vlaamse Instelling voor Technologisch Onderzoek) research institute in their research endeavors. Notably, TIMES was reported commercial in 2010 [22]. A more recent survey conducted in 2020-2021 confirmed that the model was using a commercial interface [25]. Recent developments by the IEA-ETSAP have resulted in a version that is compatible with open-source solver CBC. In various studies conducted in different regions, including Canada, Sweden, the EU, and Denmark, TIMES has been shown to utilize 12 to 32 time-slices annually [24]. It is noteworthy that Haydt et al. [55] conducted a study focusing on the electrical sector, using 288 time slices, equivalent to a 12-day time resolution, highlighting the sensitivity of results to time resolution. Regarding data accessibility, while some publications partially present the used dataset, the overall accessibility of TIMES data remains an area of ongoing inquiry [54]. Calliope is a '*tool that makes it easy to build energy system models´* at different geographical scale. Even if the framework offers the possibility of modelling multi-year systems, we did not find a relevant publication on this topic. In fact, the model is typically employed for scenario analysis with a specific focus on the electricity system. Previous studies have used the model to investigate the phasing out of fossil and nuclear energies in a multi-regional UK power system [56]. More recently, the model has been applied to analyse a scenario of a multi-energy district in Switzerland [57]. Moreover, the model has been used with decades of weather data. However, its application has been limited to assessing the impact of inter-year variability in wind and PV on the results, rather than evaluating a transition pathway [58]. Similarly GENeSYS-MOD presents some limitations. This model is an application of the open-source energy modelling system (OSeMOSYS), itself represented as a model with a poor time discretisation and a heavy computational burden according to [23]. Löffler et al. [39] applied the model to the world by splitting it into 10 regions and most of the energy demand sectors, the time disaggregation being chosen by the user. For their application they used representative years with three days and two time slice per day. Among the open-source models with an active community, PyPSA is one of the best-performing, with a large and active community, development at the state of the art, worldwide applications, and usage not only limited to academia. A study conducted by Bartholdsen et al. [40]

centered on Germany employed a representation comprising 16 time slices for representative years. This choice was substantiated by the work of Welsch et al. [59], which demonstrated that this level of temporal granularity yields consistent results in comparison to hourly time resolution over a year. However, it is noteworthy that the utilization of a limited number of time slices may simplify the optimization of storage technologies, especially those designed for inter-month energy storage. This simplification can be viewed as a pragmatic approach to reduce the computational burden while over-simplifying the challenge of accurately integrating intermittent renewable energy sources. Furthermore, PyPSA, a modeling framework recognized for its robustness and active user community, has also been employed to investigate scenarios related to myopic transitions [50]. Hence, it is worth noting that while Calliope, OSeMOSYS, PyPSA and TIMES frameworks have the potential to be used for evaluating a transition pathway, we have not come across any publication that explicitly demonstrates their application to such cases with an hourly time resolution over significant time slices.

Hence, it appears that none of the models of Tables A.1 and A.2 fully meet all five criteria outlined in the table, topped with the additional consideration of acceptable computational time. This observation is consistent with the findings presented by Prina et al. [23] who identified two approaches for optimising the energy transition pathway based on the six criteria. The first approach involves running a snapshot model multiple times using an algorithm that optimises the transition path and validates the operability of the system. The second approach aims to extend a snapshot model to represent the entire transition pathway. However, they excluded this option due to the lack of models that met the requirements of being fast enough and easily adaptable. Therefore, they developed a new model based on the first methodology, named EPLANoptTP. It uses a multi-objective evolutionary algorithm to optimise the EnergyPLAN model [35]. To manage computational time, the number of decision variables is limited to three: photovoltaic (PV), wind turbine and battery capacities. Thus, the model does not investigate all the options (i.e. criteria (iii)).

For the aforementioned reasons, the current work opted for EnergyScope Pathway, an extension of the open-source and documented EnergyScope TD model [2] listed in Tables A.1 and A.2. The latter has an horizon time of one year and does not account for the pathway from an existing energy system to a long-term target. The pathway version extends the time horizon to decades and accounts for the pathway transition from an existing energy system to a long term target. The computational time is kept low (i.e. around a 15 minutes on a personal laptop), mostly due to keeping the linear formulation after extending the snapshot model. Limpens et al. [3] provides more detailed insights

into the modeling choices made during methodological development. In the spirit of the EnergyScope project, the code is fully open-source (under the License Apache 2.0, see repo [60]) with a collaborative documentation [6]. Compared to existing models, EnergyScope Pathway introduces a rapid computational optimisation tool for exploring diverse transition pathways within an entire energy system while maintaining high temporal precision to accurately capture the integration of intermittent renewables. To the best of our knowledge, there are potentially frameworks that could be extended to similar capabilities, but their computational time for similar case study have not been found.

A.2 EnergyScope Pathway and its linear formulation

EnergyScope Pathway is the extension of EnergyScope TD [2] that follows the snapshot approach [61], consisting in optimising the system in a target future year. The objective of this section is to present the fundamental variables and constraints of the latter based on which the former was developed. There have been formulation choices to be made but they are not discussed in the current manuscript. However, the interested reader is invited to refer to the Appendix B of [3] for further information in this regard.

A.2.1 The starting point: a scenario analysis model

Overview of the snapshot model

EnergyScope TD [2] is a model that optimises both the investment and operating strategy of a '*whole*'-energy system, encompassing electricity, heating, mobility, and non-energy sectors. According to Contino et al. [62], a model qualifies as a 'whole-energy' system when it considers all energy sectors, including the non-energy demand such as the production of plastics and other materials using feedstocks that are also considered as energy carriers, with the same level of detail.

The model's hourly resolution over a year makes it well-suited for integrating intermittent renewables. Its formulation incorporates typical days and a reconstruction method that captures different time scales from the hour to the season while accounting for the inter-weeks patterns of wind. This approach minimally affects the design while significantly reducing computational time [63]. The model investigates all the possibilities by optimising the investment decisions and hourly operations over a year, with a computational time of less than a minute on a personal laptop. This charac-

teristic was intentionally incorporated into the model design to facilitate uncertainty quantification and other studies that require numerous iterations [64].

EnergyScope TD has been successfully applied to various national energy systems, including Switzerland [2, 65], Belgium [66], Italy [67], and other European countries [68]. Furthermore, it has been extended to a multi-region energy system model [63], coupled with other energy models [69], or employed to focus on specific sectors such as the power networks of electricity, gas, and hydrogen [70].

Formulation of the snapshot model

The conceptual structure of the model is illustrated in Figure A.2: given the end-use energy demand, the efficiency and cost of energy conversion technologies, the availability and cost of energy resources, the model identifies the optimal investment and hourly operation strategies to meet the demand and minimise the total annual cost or greenhouse gas emissions of the energy system. Typically, the two objectives are integrated by placing a limit on emissions while simultaneously striving to minimize costs.

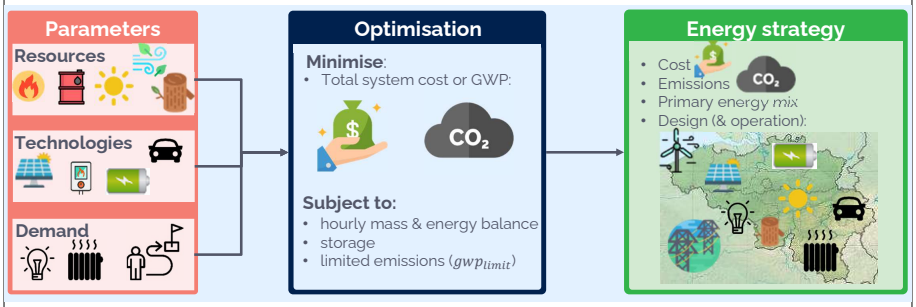

Figure A.2. EnergyScope TD model is a flow model with inputs (Parameters), an optimizing model (Optimisation) and results (Energy strategy). The image illustrates what is included (non-exhaustively).

Linear formulation

The following section illustrates, non-exhaustively, the original EnergyScope TD model. The objective function, cost and greenhouse gases (GHG) formulation will be detailed. The rest of the formulation is detailed and available in previous works [71]. This work uses the following nomenclature: SETs are in capital letters, **Variables** are in bold and with first letter capital, and *parameters* are in italic.

$$\min \ \mathbf{C_{tot}} = \sum_{j \in TECH} \left(\tau(j) \mathbf{C_{inv}}(j) + \mathbf{C_{maint}}(j) \right) + \sum_{i \in RES} \mathbf{C_{op}}(i) \tag{A.1}$$

$$\text{s.t. } \tau(j) = \frac{i_{rate}(i_{rate}+1)^{lifetime(j)}}{(i_{rate}+1)^{lifetime(j)}-1} \qquad \forall j \in TECH \tag{A.2}$$

$$\mathbf{C_{inv}}(j) = c_{inv}(j)\mathbf{F}(j) \qquad \forall j \in TECH \tag{A.3}$$

$$\mathbf{C_{maint}}(j) = c_{maint}(j)\mathbf{F}(j) \qquad \forall j \in TECH \tag{A.4}$$

$$\mathbf{C_{op}}(i) = \sum_{t \in T} c_{op}(i)\mathbf{F_t}(i,t)t_{op}(t) \qquad \forall i \in RES \tag{A.5}$$

The objective, Eq. (A.1), is the minimisation of the total annual cost of the energy system ($\mathbf{C_{tot}}$), defined as the sum of the annualised investment cost of the technologies ($\tau \cdot \mathbf{C_{inv}}$), the operating and maintenance costs of the technologies ($\mathbf{C_{maint}}$) and the operating cost of the resources ($\mathbf{C_{op}}$). The annualised factor τ is computed *a priori* based on the interest rate (i_{rate}) and the technology lifetime, (*lifetime*), Eq. (A.2). The total investment cost ($\mathbf{C_{inv}}$) of each technology results from the multiplication of its specific investment cost (c_{inv}) and its installed capacity ($\mathbf{F}$), see Eq. (A.3). The installed capacity is defined with respect to the main end-uses output type, such as electricity for PV or heat for a boiler. The total operation and maintenance costs are calculated in the same way, Eq. (A.4). The total cost of the resources is calculated as the sum of the end-use over different periods multiplied by the period duration (t_{op}) and the specific cost of the resources (c_{op}), Eq. (A.5). To simplify the reading, we write the sum over typical days as $t \in T$ such as in Eq. (A.5) and following equations. The period T represents the sequence of hours and typical days over a year (8760h)[1]. The full formulation is detailed in [2] or in the documentation [72].

$$\mathbf{GWP_{tot}} = \sum_{i \in RES} \mathbf{GWP_{op}}(i) \tag{A.6}$$

$$\mathbf{GWP_{op}}(i) = \sum_{t \in T} gwp_{op}(i)\mathbf{F_t}(i,t)t_{op}(t) \qquad \forall i \in RES \tag{A.7}$$

The global annual GHG emissions are calculated using a LCA approach, i.e. taking into account emissions of the resources '*from cradle to use*'. It is based on the indicator '*GWP100a-IPCC2013´* developed by the intergovernmental panel for climate change (IPCC) [73]. For climate change, the natural choice as indicator is the global warming potential, expressed in $ktCO_2$-eq./year. In Eq. (A.6), the total yearly emissions of the system ($\mathbf{GWP_{tot}}$) are defined as the emissions related to resources ($\mathbf{GWP_{op}}$). The total emissions of the resources are the emissions associated to fuels (from cradle to

[1] The exception is storage level which is optimised over the 365 days of the year instead of typical days.

combustion) and imports of electricity (gwp_{op}) multiplied by the period duration (t_{op}), Eq. (A.7). Thus, this version accounts only for operation without accounting for the global warming potential (GWP) emitted during the construction of the technologies. This makes the results comparable with metrics used in the reports by the European Commission and the International Energy Agency (IEA).

The above equations (Eqs. (A.1) - (A.7)) represent only a part of the formulation and illustrate the syntax that is used. Those representing the energy balance, network implementation, sectors representation, etc. are not presented in this work but are detailed in the latest version of the model, see [71] and on the documentation [72].

Finally, energy storage has two dimensions to be optimised: the stored energy quantity (also referred to as 'storage level') and the hourly power flow, encompassing both charging and discharging. EnergyScope TD optimises the hourly charge and discharge operations based on the hourly resolution of the typical days. In contrast, the optimisation of stored energy is conducted over the entire span of 8760 hours in a year. This formulation allows for the effective integration of a wide range of energy storage technologies, spanning short-term solutions like small thermal storage units and daily-use batteries, to longer-term options such as hydro-dam storage for seasonal storage, and even large-scale thermal storage for intra-week patterns. A previous study delved into the roles of various storage technologies, considering their sectoral applications and temporal aspects, within the context of the Swiss energy system [65].

A.2.2 Extending the model for pathway optimisation

In this section, we delve into the extension of EnergyScope TD from a static yearly snapshot model to a comprehensive pathway model. While snapshot models provide insights into the energy system for individual years, they lack the capacity to capture the dynamics inherent in investment strategies throughout a transition period. The proposed approach involves segmenting the transition into five-year intervals, during which the energy system is optimized for one specific year. This approach results in seven instances of EnergyScope TD – called representative years – spanning the 30-year transition period, covering the years from 2020 to 2050. To bridge these representative years, we introduce additional constraints that capture the investments changes between consecutive periods, accounting for societal inertia and evaluating both the cost implications and emissions of the transition. Overall, these constraints are integrated into a linear framework, ensuring computational efficiency, with an approximate computational time of 14 minutes on a personal laptop (2.4 GHz Intel Core i5 quad-core).

Figure A.3 illustrates the pathway concept. Simplification and choices were necessary to implement linearly the problem while keeping a tractable computational time. In this section, we present the formulation retained.

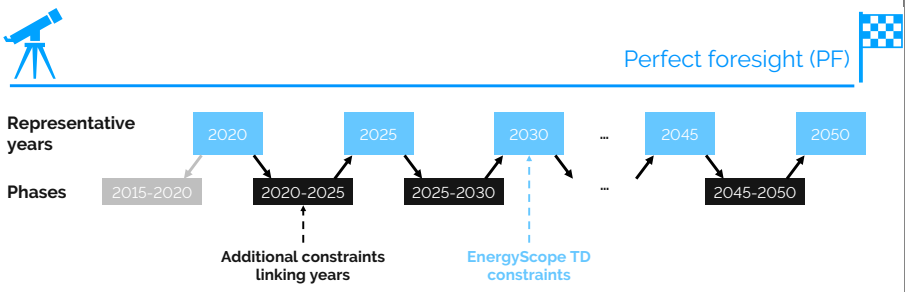

Figure A.3. The pathway methodology relies on 7 representative years (blue boxes) where the model EnergyScope Typical Days (EnergyScope TD) is applied. Moreover, the formulation accounts for linking constraints (black boxes) and an initial condition (grey box). The overall problem is the pathway model.

The proposed formulation relies on representative years, selected every 5 years from 2020 to 2050. The period between two of them is called '*PHASE´*. For each of these 7 representative years, the EnergyScope TD model is run using the relevant data (such as energy demand, technology costs or GHG emissions constraints).

As a consequence, a new dimension '*year*' is added to all **Variables** and parameters, except the interest rate (i_{rate}) assumed constant during the transition. This new dimension is necessary to represent the changes of technology and resource characteristics over the representative years. As an example, the investment cost (c_{inv}) of a solar photovoltaic panels could drastically vary in the next decades (e.g. data used ranges between 1220 to 870 [$€_{2015}$/kW] between 2020 and 2035).

Linking years

At this stage, all years are independent. In the following, we introduce new constraints to link representative years. The formulation allows to install new capacity ($\mathbf{F_{new}}$), remove a capacity that has reached its lifespan ($\mathbf{F_{old}}$) or decommission a technology prematurely ($\mathbf{F_{decom}}$). These capacity changes occur during a phase, this implies that there is no capacity change during a representative year. Figure A.4 illustrates the concept.

$$\mathbf{F}(y_{\text{stop}}, i) = \mathbf{F}(y_{\text{start}}, i) + \mathbf{F_{new}}(p, i) - \mathbf{F_{old}}(p, i) - \sum_{p2 \in PHASE \cup \{2015\_2020\}} \mathbf{F_{decom}}(p, p2, i)$$

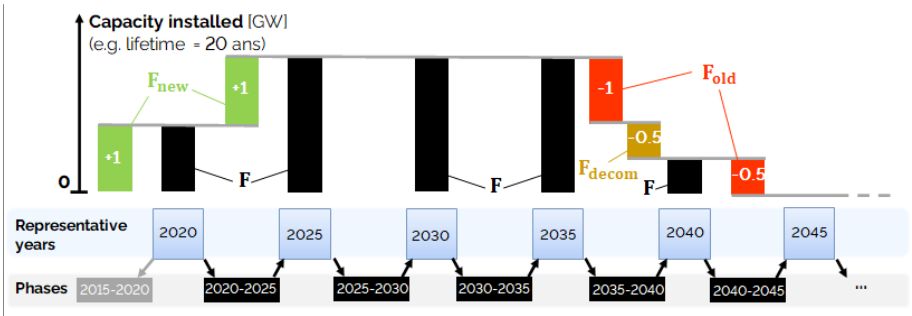

Figure A.4. Example of how the technologies capacity and associated variables are evolving. The example uses a technology with a 20 years lifetime. Initially 1 GW of capacity exists ($\mathbf{F_{new}}$ during phase 2015_2020). Then another 1 GW is deployed ($\mathbf{F_{new}}$ during phase 2020_2025). 15 years later, a part of the capacity reaches its lifetime limit and is removed ($\mathbf{F_{old}}$ phase 2035_2040). Moreover, during the latter phase, additional capacity is decommissioned prematurely ($\mathbf{F_{decom}}$). Finally, the technology reaches its expected lifetime and is fully withdrawn ($\mathbf{F_{old}}$).

$$\forall p \in PHASE, y_{stop} \in Y\_STOP(p), y_{start} \in Y\_START(p), i \in TECH \quad \text{(A.8)}$$

Similarly to a mass balance, Eq. (A.8) is the technology capacity balance. The constraint forces the installation or withdrawing of capacities between two representative years: at the end of the phase (y_{stop}), the available capacity is the one used in the next representative year ($\mathbf{F}(y_{stop})$). This capacity is equal to the one available in the previous representative year ($\mathbf{F}(y_{start})$) plus the new installed capacity ($\mathbf{F_{new}}$) minus the capacity that has reached its lifetime ($\mathbf{F_{old}}$) minus the early decommissioned capacity ($\mathbf{F_{decom}}$). One notices that the capacity available for each representative year depends on a year (y_{start} or y_{stop}), while the other capacity changes depend on a phase (p or $p2$). Moreover, the decommissioning term depends on another phase, which is the one when the technology decommissioned has been built. As an illustration, Figure A.4 gives an example where 0.5 GW of a capacity built in 2015_2020 is decommissioned in 2030_2035 ($\mathbf{F_{decom}}$(2030_2035,2015_2020,i)).

$$\mathbf{F_{decom}}(p, p2, i) = 0$$
$$\forall i \in TECH, p \in PHASE, p2 \in PHASE \cup \{2015\_2020\} | decom_{allowed}(p, p2) = 0 \quad \text{(A.9)}$$

$$\mathbf{F_{old}}(p,i) = \quad \text{if}(age = \}STILL\_IN\_USE') \text{ then } 0$$
$$\text{else } \left(\mathbf{F_{new}}(age,i) - \sum_{p2 \in PHASE} \mathbf{F_{decom}}(p2,age,i) \right)$$
$$\forall p \in PHASE, \forall j \in TECH | age \in AGE(p,j) \quad \text{(A.10)}$$

In linear programming, a solution might be mathematically correct, while not making sense in practice. As an example, a technology could be decommissioned before being built ($p < p_{built}$). Eqs. (A.9-A.10) allow preventing these non-sense while keeping the formulation linear. Eq. (A.9) forces the decommissioned capacity to zero when technology will be built after. To do so, a parameter ($decom_{allowed}$) is defined *a priori* and is equal to 0 or 1 when decommissioning is not possible or possible, respectively. Eq. (A.10) defines the capacity reaching its lifetime limit at a certain phase, the concept is illustrated in Figure A.4. For each phase, a set (*AGE*) is calculated *a priori*. It relates, for a given phase and technology, when the technology should have been built. In the case the technology has already reached its lifetime limit, the set (*AGE*) returns the phase when the technology has been built. The first part of Eq. (A.10) indicates that the technology is still available, and thus no capacity needs to be removed. The second part of the equation represents the capacity that reached its expected lifetime minus a part of the capacity that would have been decommissioned. As an example, Figure A.4 shows a 20 years lifetime technology with 1 GW of capacity installed before 2020. Ones will highlight the use of a 'if' in Eq. (A.10), this formulation is linear as the if is applied to a parameter and not a variable.

$$\mathbf{F_{new}}(2015\_2020, i) = \mathbf{F}(YEAR\_2020, i) \qquad \forall i \in TECH \quad \text{(A.11)}$$

To initialise the problem in 2020 with the existing design, an additional phase '*2015_2020*' is created. Eq. (A.11) requires that the capacity used in 2020 is installed in the previous phase.

Society inertia

To avoid unrealistically fast changes in the system, additional constraints are needed during the phases for the mobility and low temperature heat sectors. Without the following constraints, the model would eliminate certain technologies in one phase, such as oil and gas decentralised boilers. Even if this result is mathematically and physically correct, (i.e. fuels are expensive and investing in more efficient technology is economically and environmentally more profitable), this swap of technology cannot occur in one phase (i.e. 5 years). Indeed, society inertia to change, available manpower, supply chains and manufacturers limit the change.

$$\Delta_{\mathbf{change}}(p,i) \geq \sum_{t \in T} \left(\mathbf{F_t}(y_{start},i,t)\right) - \sum_{t \in T} \left(\mathbf{F_t}(y_{stop},i,t)\right)$$
$$\forall j \in TECH, p \in PHASE, y_{start} \in Y\_START(p), y_{stop} \in Y\_STOP(p) \quad \text{(A.12)}$$

$$\sum_{i \in TECH(HeatLowT)} \Delta_{\mathbf{change}}(p,i) \leq lim_{LT,ren} \cdot \left(eui(y_{start}, HotWater) + eui(y_{start}, SpaceHeat)\right)$$
$$\forall p \in PHASE, y_{start} \in Y\_START(p) \quad \text{(A.13)}$$

$$\sum_{i \in TECH(MobPass)} \Delta_{\mathbf{change}}(p,i) \leq lim_{MobPass} \cdot eui(y_{start}, MobPass))$$
$$\forall p \in PHASE, y_{start} \in Y\_START(p) \quad \text{(A.14)}$$

$$\sum_{i \in TECH(MobFreight)} \Delta_{\mathbf{change}}(p,i) \leq lim_{MobFreight} \cdot eui(y_{start}, MobFreight)$$
$$\forall p \in PHASE, y_{start} \in Y\_START(p) \quad \text{(A.15)}$$

Eq. (A.12) calculates the upper limit of change ($\Delta_{\mathbf{change}}$) in terms of supplied demand instead of installed capacity. Based on this quantification, the amount of change per phase is limited for low temperature heat ($lim_{LT,ren}$), Eq. (A.13), passenger mobility ($lim_{MobPass}$), Eq. (A.14) and freight mobility ($lim_{MobFreight}$), Eq. (A.15). For instance, if the maximum allowable variation in supplied low temperature heat is set at 25%, it would restrict the technology-related changes in low temperature heat to 25% within a given phase. Consequently, if a technology supplies more than 25% of the low temperature heat, it would require multiple phases to replace it with a different technology.

Cost and emissions of the transition

To optimise the energy system, two key metrics must be adapted: the transition cost and the total global warming potential (GWP). Concerning the first one, all costs are expressed in $€_{2015}$ and an annualisation factor is used to distinguish investments over the transition. For the GWP, the metric used is based on the contributions of the gases over 100 years. It is assumed that the impact of emitting at the beginning or the end of transition are equivalent and thus no annualisation is used.

$$\min \ \mathbf{C_{tot,trans}} = \mathbf{C_{tot,capex}} + \mathbf{C_{tot,opex}} \tag{A.16}$$

$$\mathbf{C_{tot,capex}} = \sum_{p \in PHASE \cup \{2015\_2020\}} \mathbf{C_{inv,phase}}(p) - \sum_{i \in TECH} \mathbf{C_{inv,return}}(i) \tag{A.17}$$

$$\mathbf{C_{tot,opex}} = \mathbf{C_{opex}}(2020) + t_{phase} \cdot \tau_{phase}(p) \cdot \sum_{p \in PHASE | y_{\text{start}} \in P\_START(p), y_{\text{stop}} \in P\_STOP(p)} \Big(\mathbf{C_{opex}}(y_{\text{start}}) + \mathbf{C_{opex}}(y_{\text{stop}}) \Big) / 2 \tag{A.18}$$

$$\tau_{phase}(p) = 1/(1 + i_{rate})^{diff\_2015\_year(p)} \tag{A.19}$$

The objective function to be minimised is the total transition cost of the energy system ($\mathbf{C_{tot,trans}}$), defined as the sum of the total capital expenditure (CAPEX) ($\mathbf{C_{tot,capex}}$) and the operational expenditure (OPEX) ($\mathbf{C_{tot,opex}}$), according to Eq. (A.16). The total CAPEX ($\mathbf{C_{tot,capex}}$) is the sum of the investment during each phase ($\mathbf{C_{inv,phase}}$), Eq. (A.17), to which the residual asset investment cost in 2050 is withdrawn ($\mathbf{C_{inv,return}}$). Thus, the investments account for the installation and dismantlement costs of the technologies. The total OPEX ($\mathbf{C_{tot,opex}}$) is the sum of the OPEX in 2020 and the annualised sum of the OPEX during each phase ($\mathbf{C_{opex}}$), Eq. (A.18). During a phase, the system OPEX is the product of the annualised phase factor, defined in Eq. (A.19), and the arithmetic average of OPEX cost for the representative years before and after the phase. The annualised phase factor is defined based on an average interest rate during the transition.

$$\mathbf{C_{opex}}(y) = \sum_{i \in TECH} \mathbf{C_{maint}}(y, i) + \sum_{j \in RES} \mathbf{C_{op}}(y, j) \qquad \forall y \in YEARS \tag{A.20}$$

For each year, the yearly OPEX ($\mathbf{C_{opex}}$) is the sum of the operating and maintenance costs of technologies ($\mathbf{C_{maint}}$) and the operating cost of the resources ($\mathbf{C_{op}}$), Eq. (A.20).

$$\mathbf{C_{inv,phase}}(p) = \sum_{j \in TECH} \mathbf{F_{new}}(p, j) \cdot \tau_{phase}(p) \cdot \left(c_{inv}(y_{start}, j) + c_{inv}(y_{stop}, j) \right) / 2$$
$$\forall p \in PHASE | y_{\text{start}} \in P\_START(p), y_{\text{stop}} \in P\_STOP(p) \tag{A.21}$$

The investment during a phase ($\mathbf{C_{inv,phase}}$) results from the multiplication of the newly built technologies ($\mathbf{F_{new}}$) with their annualised arithmetic averaged specific cost, Eq. (A.21). The annualised phase factor (defined by Eq. (A.19)) is used. The specific cost during the phase is defined as the average between the investment cost for the first and last year of the period.

$$\mathbf{C_{inv,return}}(i) = \sum_{p \in PHASE \cup \{2015\_2020\} | y_{\text{start}} \in Y\_START(p), y_{\text{stop}} \in Y\_STOP(p)} \tau_{phase}(p) \cdot \left(c_{inv}(y_{start}, i) + c_{inv}(y_{stop}, i)\right) /2 \cdot \frac{remaining\_years(i,p)}{lifetime(y_{\text{start}}, i)} \left(\mathbf{F_{new}}(p,i) - \sum_{p2 \in PHASE} \mathbf{F_{decom}}(p2,p,i) \right) \quad \forall i \in TECH \tag{A.22}$$

A part of the investment will remain after 2050. This residual investment, also called salvage value, can be calculated for each technology. A parameter, calculated *a priori* , gives for each technology and construction phase, the remaining amount of years (*remaining_years*). As an example, if a PV panel has been built in 2045 and has a 20 years lifetime, the parameter will equal to 15 years. Thus, the salvage value is a fraction of the investment cost of this technology when it has been built. This fraction is the ratio between the number of remaining years and the lifetime of the technology. In the previous example, the residual investment of the PV built is 75%. Eq. (A.22) computes, for each technology, the residual value that must be deducted from the total cost. The residual value reflects the fact that the technology can still be used after the horizon of the model and is not fully amortised. The residual value is not applied to technologies that are removed prematurely. This differ from other models, such as Plexos where a technology removed prematurely will benefit from its salvage value (see analysis of [47]).

$$\mathbf{GWP_{tot,trans}} = \mathbf{GWP_{tot}}(2020) + t_{phase} \sum_{p \in PHASE | y_{\text{start}} \in Y\_START(p), y_{\text{stop}} \in Y\_STOP(p)} /2 \left(\mathbf{GWP_{tot}}(y_{\text{start}}) + \mathbf{GWP_{tot}}(y_{\text{stop}})\right) \tag{A.23}$$

$$\mathbf{GWP_{tot,trans}} \leq gwp_{lim,trans} \tag{A.24}$$

The total global warming potential (GWP) emissions during the transition ($\mathbf{GWP_{tot,trans}}$) are equal to the sum of the total emissions per period ($\mathbf{GWP_{tot}}$), Eq. (A.23). The emissions during a phase is estimated as the arithmetic average of the representative years before and after the phase. Eq. (A.24) limits the total GWP emissions during the transition by a maximum ($gwp_{lim,trans}$).

Appendix B

Case study: the Belgian energy system

B.1 Belgian energy system in 2020

The Belgian whole-energy system of 2020 was largely based (88.6% of the primary energy mix) on “conventional fuels"(i.e. oil and oil products (38.2%), natural gas (29.5%), uranium (16.3%) and solid fossil fuels (4.6%) while the rest mainly accounts for 26.7 TWh of lignocellulosic and wet biomass, 12.8 TWh of wind and 5.1 TWh of solar [74]. Given the data available in the literature (mostly for the power sector) and, when not available, following the assumptions made by Limpens et al. [66], Table B.1 gives the major technologies used in 2020 to supply the different demands of **??**.

B.2 Belgian energy transition pathway towards carbon-neutrality in 2050

This section presents the results of the deterministic (i.e. all parameters at their respective nominal value) perfect foresight optimisation of the Belgian energy transition pathway constrained to a linear decrease of the GHG emissions from 2020 (121 $MtCO_{2,eq}$) to carbon-neutrality in 2050. After performing a technical investigation of the pathway by checking the greenhouse gas breakdown by energy sectors, the primary energy mix is analysed. To illustrate the sector coupling, a focus is made on the electrification of other sectors. Then, the cost implications in terms of investments and operations are discussed.

Table B.1. Major technologies used to supply the 2020-demands of **??** in terms of share of production and installed capacity.

End-use demand	**Major technologies**	**Share of supply**	**Installed capacity**
Electricity	Nuclear	39%	5.9 GW
	CCGT	21%	3.9 GW
	Wind turbines	14%	5.0 GW
Heat High-Temp.	Gas boiler	36%	3.3 GW
	Coal boiler	30%	2.3 GW
	Oil boiler	20%	1.5 GW
Heat Low-Temp. (DEC)[a]	Oil boiler	48%	21.4 GW
	Gas boiler	40%	17.5 GW
	Wood boiler	10%	4.4 GW
Heat Low-Temp. (DHN)	Gas CHP	59%	0.3 GW
	Gas boiler	15%	0.3 GW
	Waste CHP	15%	0.1 GW
Private mobility[b]	Diesel car	49%	93.5 Mpass.-km/h
	Gasoline car	49%	94.7 Mpass.-km/h
	HEV	2%	5.9 Mpass.-km/h
Public mobility	Diesel bus	43%	3.6 Mpass.-km/h
	Train	43%	3.9 Mpass.-km/h
	CNG bus	5%	0.8 Mpass.-km/h
Freight mobility	Diesel truck	74%	62.7 Mt.-km/h
	Diesel boat	15%	10.8 Mt.-km/h
	Train	11%	2.5 Mt.-km/h
HVC	Naphtha/LPG cracking	100%	4.6 GW
Ammonia	Haber-Bosch	100%	1 GW
Methanol	Import	100%	-

[a] The decentralised heating units provide 98% of the low-temperature heat demand.
[b] The private mobility accounts for 80% of the passengers mobility.

B.2.1 Greenhouse gases and primary energy

Figure B.1 shows the greenhouse gases (GHG) per sector. The system reaches its upper bound (i.e. maximum emissions) every year.

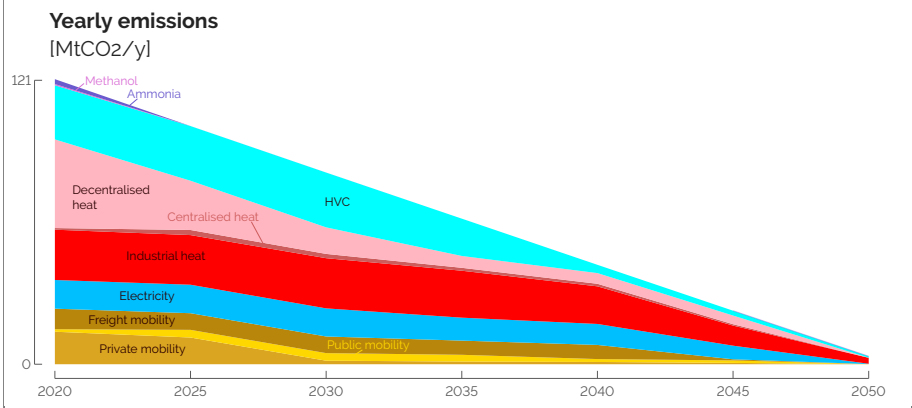

Figure B.1. Energy sectors have different speed to reduce GHG emissions over the transition. The system uses all the allowed GHG prescribed by the linear decrease from the emissions in 2020 until carbon-neutrality in 2050.

The defossilisation[1] of the different sectors are not performed at the same rate. The non-energy demand of methanol and ammonia are substituted by electrofuels. These are the first use of electrofuels as e-ammonia is the cheapest electrofuel thanks to the high maturity of the Haber-Bosch process. The decentralised heat and mobility sectors are also dropping first. This is a combination of efficiency and substitution of fossil fuels with electricity. Efficiency comes mainly from district heating networks and electrical heat pumps for the heat sector, and public mobility and electric cars for the mobility sector. From 2040 onward, the decreases are mainly due to the substitution of the remaining fossil fuels by electrofuels as illustrated in Figure B.2.

Figure B.2 shows the primary energy mix for the different representative years. The pathway verifies five trends: (i) reduction of primary energy thanks to energy efficiency; (ii) massive integration of endogenous renewable energies; (iii) importance of electrification; (iv) the usage of gas as the last fossil resource; and (v) the obligation to rely on renewable fuels to achieve carbon neutrality.

[1] In a more sustainable future, some of the energy carriers, currently produced mostly from fossil resources, will still consist of hydrocarbons (e.g. e-methane or e-methanol). This is why this paper rather uses "defossilisation" rather than "decarbonisation" as carbon will still play a key role in a carbon-neutral energy transition [75].

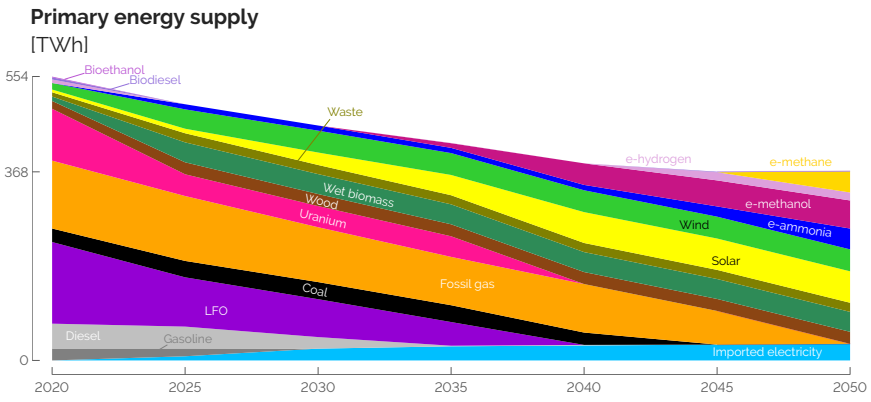

Figure B.2. Primary energy emitting GHG (below Uranium) are reducing linearly with fossil gas remaining until 2045. A part of this energy is replaced by renewable ones and starting from 2040, a significant share of electrofuels. As end-use demands slightly increase (see Figure **??**), the drop represents energy efficiency (i.e. providing the same services with less primary energy).

The energy supply decreases from 554 TWh/y in 2020 down to 368 TWh/y in 2050 (i.e. -34%) whereas, in the meantime, the demands have increased by 19%, on average. This drop of primary energy consumption reflects the penetration of efficient measures and technologies, such as the previously mentioned public mobility, DHN or heat pumps. The results in 2050 are aligned with other studies, such as Devogelaer et al. [76][2] and My2050[3] [78] which estimates respectively a range of 305-417 TWh/y and 307-364 TWh/y for their central scenarios.

The first fossil energy to phase out is gasoline, which is exclusively used for private cars. Indeed, private mobility is partially replaced by public one[4]; and the cars are switching from gasoline and diesel to electricity. Then, diesel and light fuel oil (LFO) are decreasing. As diesel is used for trucks and buses mobility, it is harder to phase out compared to gasoline exclusively burned in cars. The first drop of LFO reflects the switch from oil boilers to other technologies: heat pumps and gas cogeneration mainly.

[2]This study was ordered by the National Planning Bureau in 2013. Five scenarios are proposed.

[3]The Climate Change Service of the Federal Public Service Health launched an initiative in 2012 entitled '*Low Carbon Belgium by 2050*'. This initiative resulted in a report and a calculator in 2013 [77]. The Belgian calculator has been improved since then into a recent expert version called **My2050** [78]. From this study, the results of two scenarios will be used: one based on an optimistic evolution of technologies (Technology), and one focusing on an increased dependence on neighbouring countries (EU integration).

[4]Given the major role played by private cars in the Belgian passenger mobility nowadays (i.e. around 80% [79]), public transport (e.g. tramways, buses and trains) is assumed to be able to supply only half of it.

Then, it is mainly used for the production of high value chemicals (HVC), this reflects that HVC is a feedstock hard to defossilise. Finally, coal is kept mainly for industrial usage because it is a cheap fossil fuel (mainly for industrial usage). To phase it out beforehand, a penalty mechanism, such as a carbon tax, would be required, or its strict ban should be put in place. The last fossil energy present in the system is fossil gas, used for the production of electricity and heat, through cogeneration mainly. Indeed, gas plays a key role to balance the intermittency of solar and wind.

The consumption of uranium declines in 2025, dropping to 2 GW, primarily due to the political framework aimed at phasing out nuclear energy [80]. In the initial stages, significant deployment of endogenous energies takes place. This includes the utilization of wood, wet biomass, and wind energy, followed by the introduction of solar energy. However, solar energy is not fully deployed during this period due to higher integration costs. Starting from 2025, the importation of electrofuels begins, although their significant utilisation is observed from 2035 onwards. Initially, these fuels are predominantly employed as feedstocks in non-energy sectors. From 2040, e-methanol is additionally utilised for the production of High-Value Chemicals (HVCs), e-hydrogen is employed for mobility purposes, and both e-methane and e-ammonia are used for electricity generation through gas combined heat and power (CHP) and ammonia-based combined cycle gas turbine (CCGT) plants (see Figure B.3).

In 2020, Belgium has been a net-exporter of electricity, however with the shut-down of nuclear power plants and the increase of electricity consumption, Belgium will become a net importer of electricity. These imports reach their maximal allowed capacity by 2035 (i.e. 30% of electricity end use). This strong dependence on imported electricity illustrates the need for balancing intermittent renewables without relying on fossil fuels.

B.2.2 Electricity sector: Capacities and yearly balance

To better understand the electricity sector, the installed production capacities are given in Figure B.3, while the supply-demand yearly balance is illustrated in Figure B.4.

As introduced in the primary energy analysis (see Figure B.2), renewable capacities soar. By 2050, wind and solar technologies deployments are 60 GW of PV, 10 GW of onshore wind turbines and 6 GW of offshore wind turbines. To compensate the intermittency, the system relies on imported electricity, gas CCGT, sector coupling and storage. As an illustration, in 2050, 176.8 TWh of electricity transit on the grid which includes 32.4 TWh of electricity imported and 15.4 TWh of electricity from CCGT. This result is aligned with other studies that estimates different ranges: 180-310 TWh/y

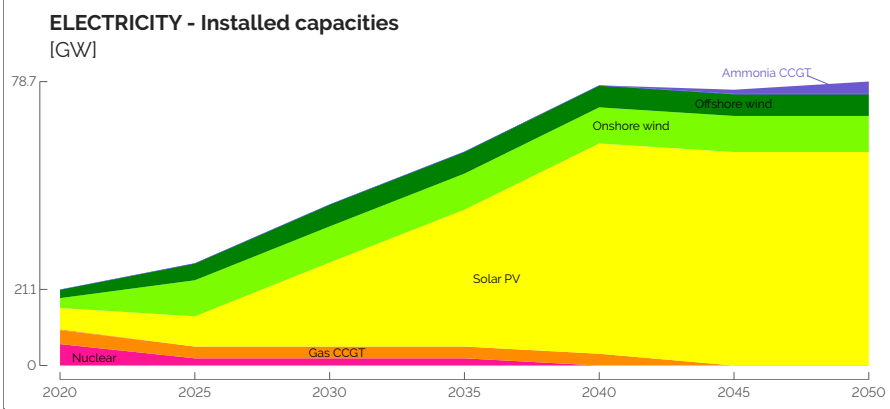

Figure B.3. The electrical production capacity will experience massive expansion of wind turbines (onshore and then offshore) and a soaring installed capacity of PV. Ammonia CCGT are installed at the end of the transition to provide a flexible capacity as gas CCGT are phased out.

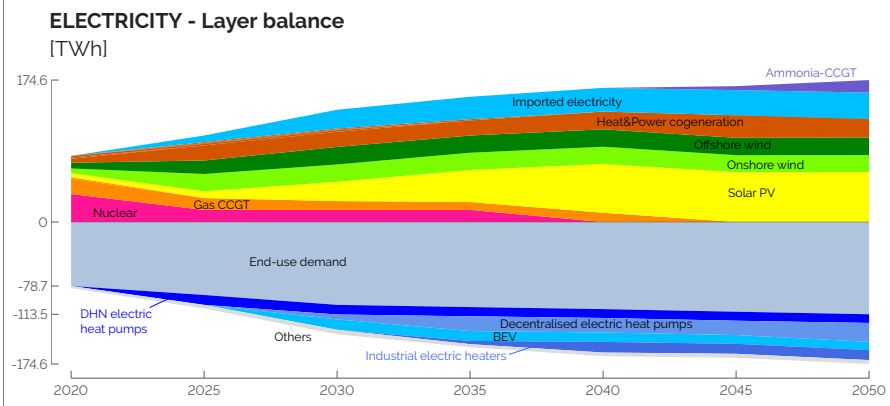

Figure B.4. The electricity supply (positive values) will remain a mix of different technologies where backup is first mainly provided by gas-CCGT and then imported electricity, heat and power cogeneration and later ammonia-CCGT. The electricity demand (negative values) is led by the electricity end-use demand, but the share used to electrify heat (heat pumps), vehicles (cars, trains, trams, ...) and industrial heaters drastically increase. This enables a flexible demand that can facilitate the integration of intermittent renewables.

[76], 126-140 TWh/y [78] and in a more recent study using the TIMES-BE model, 185-196 TWh/y [81]. Higher values from Devogelaer et al. [76] illustrate an almost exclusively electrified energy system. The differences between the study ranges reflect the different assumptions in terms of renewable potentials and availability of nuclear energy. A general trend is that Belgium should maximise its use of endogenous renewable resources, which Dubois et al. [82] identified as a cheaper option than importing additional renewable energies from abroad. Demand management reflects the flexible use of electricity, mainly through heat pumps that uncouple the heat demand and the electricity consumption when combined with thermal storage. Gas CCGT is also a useful asset to compensate intermittent renewables. However, its capacity remains the same as the one installed in 2020. These results are verifying an hourly adequacy of the power demand. Moreover, in a previous study by Pavičević et al. [69], the snapshot version of the model has been coupled with Dispa-SET, a dispatch optimisation model. Results showed that the backup capacity was underestimated by less than 20% to respect reserve capacity, mainly due the lack of reserve capacity for grid stability.

From 2025, the electricity mix has a strong renewable share that rises up to 60% in 2050. The remaining 40% are mainly gas (or ammonia) in CCGT and cogeneration and imported electricity. From a demand perspective, the electrification first starts with DHN heat pumps, then electric cars, then decentralised heat pumps and finally industrial heaters. The latter reflects the usage of cheap PV production peaks.

B.2.3 Costs: Investments and operation

In the following paragraphs, the results are analysed from an economic perspective to decipher the choices made by the model, as the overall cost of the transition is 1 004 b$€_{2015}$ split unequally among the sectors.

Figure B.5 illustrates the cumulative investments made throughout the transition, amounting to a total of 377.8 b$€_{2015}$. Initially, the infrastructure, transport, and electricity sectors each account for approximately one-third of the investments. The investments in infrastructure are primarily driven by the electricity grid and the district heating network (DHN), representing a combined investment of 73 b$€_{2015}$. The electricity sector's investment is led by power plants, totalling 31.5 b€. Notably, the investment costs in the mobility sector are primarily attributed to private cars, constituting 71% of the total. A rough estimation confirms the significant investment in cars, with an average of 500,000 vehicles registered annually in Belgium over the last decade [83] and assuming an average cost of 20 k€ per car, the funds allocated to private cars amount to 10 b€ per year. This trend in private cars explains why the private mobility sector

accounts for half of the investments required to achieve the transition by 2050. This finding aligns with other studies, such as Devogelaer et al. [76], which estimates cumulative investment expenditures of approximately 600 b€$_{2005}$ for the transport sector between 2013 and 2050, which confirms our conservative approach in the estimation.

As a comparison, the investments required to fully deploy the PV and wind potentials from 2020 to 2050 amount to 74.4 b€$_{2015}$, with an additional 22.2 b€$_{2015}$ allocated to reinforce the grid. The electrification of the heating sectors necessitates investments of 29.2 b€$_{2015}$, including 6.5 b€$_{2015}$ for the deployment of the DHN infrastructure. Storage investments, primarily focused on DHN seasonal storage, amount to 3.6 b€$_{2015}$. Apart from the investment required to replace all private vehicles (accounting for 44% of the overall investments), the remaining sectors represent a total of 212 b€$_{2015}$. To mitigate the cost of the transition, My2050 suggests deploying a fleet of no more than one million vehicles and implementing a car sharing system, distinct from car-pooling, as an inevitable measure [78].

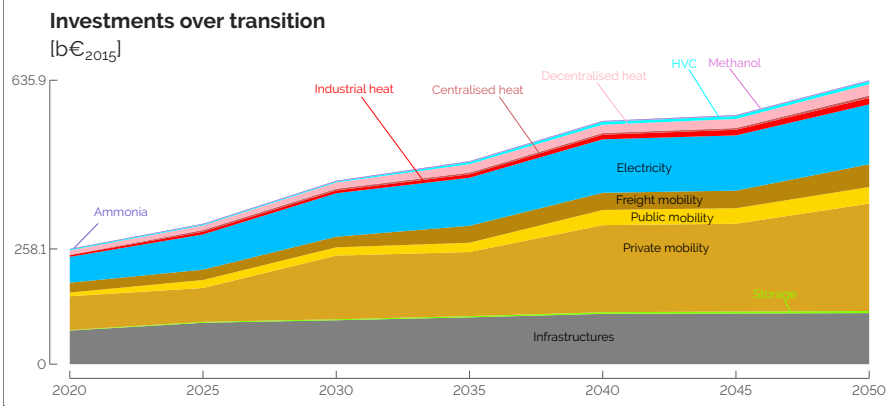

Figure B.5. The cumulative investments over the transition is unequally spread between the sectors. The energy system in 2020 is imposed to the existing energy system and its expenses are split in three main categories: mobility (mainly vehicles), infrastructure (mainly grids) and electricity (mainly thermal power plants). The investments required during the transition represents 150% the initial investment and mainly in the same three sectors.

A part of the investment will be recovered at the end of the transition based on the remaining lifespan of the technology after 2050. Figure B.6 illustrates the salvage value by sectors, calculated according to Eq. (A.22). Out of the 114.4 b€$_{2015}$ of investments in the infrastructure (i.e. mostly power grid and gas network), 55.9% remain available after 2050, due to their long lifetime. On the contrary, private mobility has a lower

salvage value due to a major drop within the first four years and an average lifetime below 10 years [83].

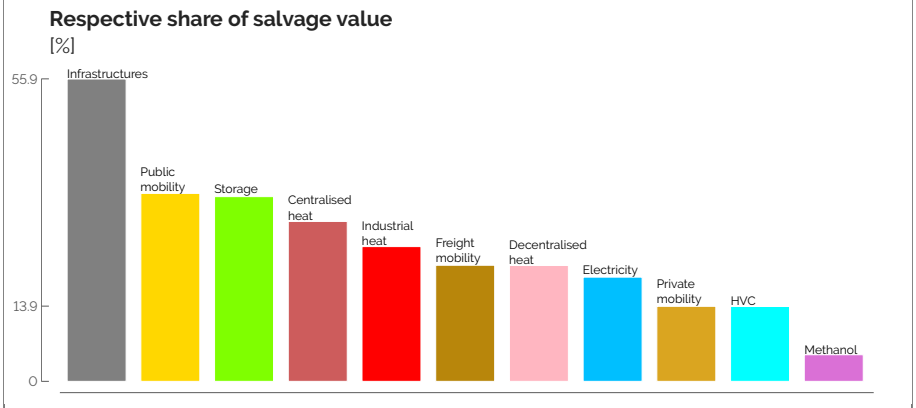

Figure B.6. By the end of the transition (i.e. in 2050), the ratio between the salvage value and its cumulative investment, per sector, is unequal. Investments in infrastructures, public mobility, storage and other long-lifetime technologies experience an important salvage value, at the contrary, investments in private mobility will not be recovered as vehicles have a short lifetime. All together, these salvage values represent 160.1 b$€_{2015}$, 25% of the cumulative investment costs in 2050.

In addition to investment decisions, the operational expenditure (OPEX), which accounts for resource utilisation and technology maintenance, are significant. Figure B.7 shows the yearly system cost for each sector except the OPEX related to resources that are grouped together. The latter dominates the OPEX, with a significant share of non-renewable resources (i.e. 63.6% in 2020) until 2040, followed by a steep increase in the share of renewable resources (i.e. 66.2% in 2050). The substantial reliance on non-renewable resources reflects the prevalent use of fossil fuels in our current energy system. The high cost-share of non-renewable fuels underscores the economic challenges of simply substituting fossil fuels with renewables, particularly evident when emphasizing that electrofuels are 2-3 times more expensive. Maintenance expenses in the private mobility sector rank second in terms of expenditure. On the other hand, maintenance expenses in other sectors are relatively small compared to the aforementioned sectors.

The annualised cost of the energy system in 2020 is estimated to 44.3 b€/y and increases by 5.5 b€/y to reach 49.8 b€/y by 2050. **My2050** estimates the annualised cost in 2050 between 63 and 82 b€/y [78], while the other studies just indicate the cost increase compared to 2015 (+11.7 to +21) [76, 81]. The differences come from the

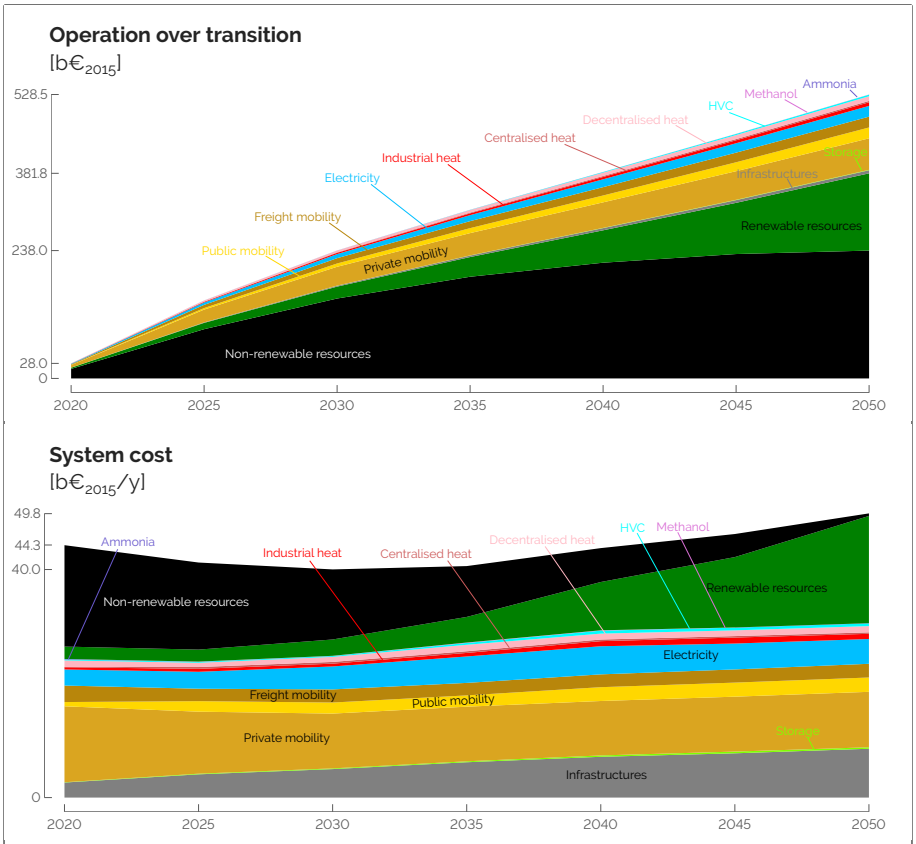

Figure B.7. The yearly system cost shows the shift from non-renewable to renewable resources (mainly electrofuels). Operation cost and maintenance represents almost 50% of the expenses.

scope of the energy system, as an example **My2050** also accounts for the agriculture sector. These differences highlight the difficulty to compare different studies due to difference of scope and partial availability of used data. Overall, comparing with existing studies shows the consistency of the results provided by EnergyScope Pathway.

B.3 CO_2-budget versus linear decrease of emissions

Figure B.8 shows the yearly emissions attributed for each sector in the REF case (i.e. imposed CO_2-budget) and a case where the CO_2-trajectory is constrained instead. Interestingly, these two transition pathways end up in a similar carbon-neutral whole-

energy system in 2050. The two main sectors that significantly reduce their emissions in the REF case are the production of HVC and the high-temperature heat. In the former, this is linked to the extended use of oil products through naphtha-cracking. The latter is produced by industrial coal boilers for longer, until 2040. Overall, ending up to the same level of emissions in 2050, the REF case represents a 60% reduction of the cumulative emissions compared to the linear decrease, for a 7.5% more expensive transition.

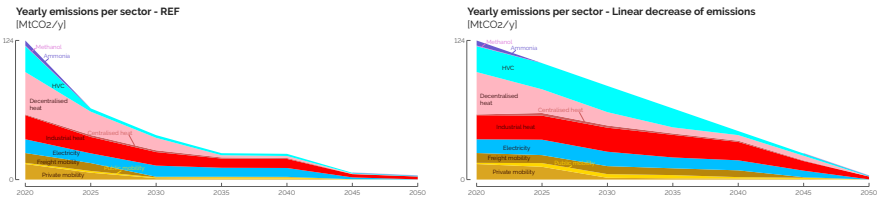

Figure B.8. Respecting the CO_2-budget imposed in the REF case drastically cuts the emissions of the system, especially in the production of high value chemicals (HVC) and the high-temperature heating sector.

B.4 Uncertainty characterisation for the 5-year steps transition

Table B.2 summarises the uncertainty ranges for the different groups of technologies and resources, for the year 2025. Refer to [5, 20] for the methodology and sources. As the model optimises the system every 5 years, $N = 5$ has been selected to get the final ranges of uncertainties of type II and III, based on the work of Moret [20]. For type III uncertainties (i.e. uncertainty ranges increasing with time), a 50% increase has been set arbitrarily between the ranges for 2025 and these same ranges for 2050. In other words, for these specific uncertainties, the ranges for 2050 are 50% larger than for 2025.

Rixhon et al. [64] analysed the impact of these parameters on the total cost of the snapshot Belgian whole-energy system in 2050 subject to different GWP limits. Based on this work, we have selected a subset of impacting uncertainties, added others due to the pathway formulation (e.g. $\Delta_{\text{change,pass}}$), and listed them in Table B.2. The uncertainty characterisation gives the uncertainty ranges per parameter or group of parameters (category).

This work considers nine groups of uncertain parameters: (i) the cost of purchasing imported energy carriers; (ii) the investment cost (i.e. CAPEX) of some technologies, mostly related to the mobility sector and the integration of renewables; (iii) the main-

tenance cost (i.e. OPEX) of every technology; (iv) the consumption of electric and fuel cells vehicles in the mobility sector; (v) the potential installed capacity of renewables; (vi) the hourly load factor of renewables accounting for variability of solar irradiance or wind speed; (vii) the availability of resources considered as limited (i.e. biomass and electricity); (viii) the end-use-demands split per sector of activities (i.e. households, services, passenger mobility and industry) and (ix) other parameters like the interest rate or the modal share change in different key sectors. For the specific case of small modular reactor (SMR), the parameter $f_{\text{max,SMR}}$ will influence the maximum capacity (i.e. 6 GW) to install to translate somehow the readiness of this technology. If it is (i) smaller than 0.6, there is no possibility to install SMR during the transition; (ii) between 0.6 and 0.8, these 6 GW can be installed only in 2050; (iii) between 0.8 and 0.9, these can be installed from 2045 onward and; (iv) higher than 0.9, the prescribed maximum capacity can be installed from 2040 onward.

Table B.2. Application of the uncertainty characterization method to the EnergyScope Pathway model for the year 2025.

Category	Parameter	Meaning	Type[a]	Relative variation[b] min	Relative variation[b] max
Cost of purchasing	$c_{op,fossil}$	Purchase fossil fuels	II	-64.3%	179.8%
	$c_{op,elec}$	Purchase electricity	II	-64.3%	179.8%
	$\boldsymbol{c_{op,electrofuels}}$	**Purchase electrofuels**	**II**	**-64.3%**	**179.8%**
	$c_{op,biofuels}$	Purchase biofuels	II	-64.3%	179.8%
Investment cost	$c_{inv,car}$	CAPEX car	I	-21.6%	25.0%
	$c_{inv,bus}$	CAPEX bus	I	-21.6%	25.0%
	c_{inv,ic_prop}	CAPEX ICE	I	-21.6%	25.0%
	c_{inv,e_prop}	CAPEX electric motor	I	-39.6%	39.6%
	c_{inv,fc_prop}	CAPEX fuel cell engine	I	-39.6%	39.6%
	$c_{inv,efficiency}$	CAPEX efficiency measures	I	-39.3%	39.3%
	$c_{inv,PV}$	CAPEX PV	I	-39.6%	39.6%
	$c_{inv,grid}$	CAPEX power grid	I	-39.3%	39.3%
	$c_{inv,grid\_enforce}$	CAPEX grid reinforcement	I	-39.3%	39.3%
	$\boldsymbol{c_{inv,nuclear\_SMR}}$	**CAPEX SMR**[c]	**I**	**-40.0%**	**44.0%**
Maintenance cost	$c_{maint,var}$	Variable OPEX of technologies	I	-48.2%	35.7%
Consumption	η_{e_prop}	Consumption electric vehicles	I	-28.7%	28.7%
	η_{fc_prop}	Consumption fuel cell vehicles	I	-28.7%	28.7%
Potential installed capacity	$f_{max,PV}$	Max capacity PV	I	-24.1%	24.1%
	$f_{max,windon}$	Max capacity onshore wind	I	-24.1%	24.1%
	$f_{max,windoff}$	Max capacity offshore wind	I	-24.1%	24.1%
Hourly load factor	$c_{p,t,PV}$	Hourly load factor PV	II	-22.1%	22.1%
	$c_{p,t,winds}$	Hourly load factor wind turbines	II	-22.1%	22.1%
Resource availability	$avail_{elec}$	Available electricity import	I	-32.1%	32.1%
	$avail_{biomass}$	Available local biomass	I	-32.1%	32.1%
End-use demand	HH_EUD	Households EUD	III	-13.8%	11.2%
	$services\_EUD$	Services EUD	III	-14.3%	11%
	$pass\_EUD$	Passenger mobility EUD	III	-7.5%	7.5%
	$industry\_EUD$	Industry EUD	III	-20.5%	16.0%
Miscellaneous	i_{rate}	Interest rate	I	-46.2%	46.2%
	$\%_{pub,max}$	Max share of public transport	I	-10%	10%
	$\Delta_{change,freight}$	Modal share change freight mobility	-	-30%	30%
	$\Delta_{change,pass}$	Modal share change passenger mobility	-	-30%	30%
	Δ_{change,LT_heat}	Modal share change LT-heat	-	-30%	30%
	$\boldsymbol{f_{max,SMR}}$	**Potential capacity SMR**	**-**	**0**	**1**

[a] Per [20], "I: investment-type, II: operation-type (constant uncertainty over time), III: operation-type (uncertainty increasing over time)".

[b] The nominal values of each of the parameters is 0, meaning no variation compared to the nominal values of the impacted parameter in the model.

[c] This range has been inferred from the local sensitivity analysis performed by EnergyVille [81].